



HAL
open science

Hydrophobe-free miniemulsion polymerization: towards high solid content of fatty acid-based poly(urethane-urea) latexes

Estelle Rix, Ceglia Gaétane, Julien Bajt, Guillaume Chollet, Valérie Héroguez, Etienne Grau, Henri Cramail

► To cite this version:

Estelle Rix, Ceglia Gaétane, Julien Bajt, Guillaume Chollet, Valérie Héroguez, et al.. Hydrophobe-free miniemulsion polymerization: towards high solid content of fatty acid-based poly(urethane-urea) latexes. *Polymer Chemistry*, 2015, 6 (2), pp.213-217. 10.1039/c4py00960f . hal-01366380

HAL Id: hal-01366380

<https://hal.science/hal-01366380v1>

Submitted on 26 Nov 2019

HAL is a multi-disciplinary open access archive for the deposit and dissemination of scientific research documents, whether they are published or not. The documents may come from teaching and research institutions in France or abroad, or from public or private research centers.

L'archive ouverte pluridisciplinaire **HAL**, est destinée au dépôt et à la diffusion de documents scientifiques de niveau recherche, publiés ou non, émanant des établissements d'enseignement et de recherche français ou étrangers, des laboratoires publics ou privés.

Hydrophobe-free miniemulsion polymerization: towards high solid content of fatty acid-based poly(urethane-urea)s latexes

E. Rix,^{ab} G. Ceglia,^{ab} J. Bajt,^{ab} G. Chollet,^c V. Heroguez,^{ab} E. Grau^{ab} and H. Cramail^{*ab}

Polyurethane-urea latex particles were synthesized by miniemulsion polyaddition of fatty acid-based diol derivatives and isophorone diisocyanate. The influence of the solid content, the surfactant and the hydrophobic agent was studied. Stable monodispersed latex particles with diameters around 200-300nm were obtained with solid content up to 50wt%, without use of any additional hydrophobic agent.

Due to the depletion of fossil carbon resources, biomass as a sustainable resource is gaining importance. Among them, vegetable oils are interesting molecules for polymer synthesis through the derivatization of their functional groups.¹⁻⁶ They are easily turned into diols or polyols that can be used for the synthesis of polyurethanes (PU).⁷⁻¹² Moreover, the literature also describes few examples of vegetable-based diisocyanates.¹³⁻¹⁵

Polyurethanes are commodity polymers that are used in a wide range of applications, from foams to textile fibers or glues. Polyurethane latexes are interesting for coating and adhesive applications. Most aqueous PU dispersions are made *via* the commonly called “acetone process”.¹⁶ The principle is to polymerize in a volatile organic solvent, usually acetone, and to subsequently disperse the polymer mixture in water and then to evaporate the organic solvent. This enables the production of non-VOC aqueous PU dispersions. Recent works use vegetable-based polyols^{17,18} from triglycerides and also vegetable-based diisocyanates^{19,20} to get fully biobased PU. Still, this method uses organic solvents.

A greener route to non-VOC aqueous PU dispersions can be through miniemulsion polymerization. It was initially designed for radical polymerizations but the polymerization mechanisms have been extended over the years. In 2000, Landfester *et al.* were the first to describe polyadditions by miniemulsion polymerization with bis-epoxides and diamines.²¹ They further described the miniemulsion polyaddition of isophorone diisocyanate (IPDI) and 1,12-dodecanediol using hexadecane as a hydrophobic agent.²² The polyurethane latexes obtained with solid contents around 20wt% exhibit particle sizes around 200 nm. More recently, Chiu *et al.* produced high molecular weight PU by miniemulsion polymerization of IPDI and poly(tetramethylene oxide).²³ The

authors obtained large particles around 800-900nm with molecular weights up to 26 kg/mol but did not report the solid content. Other works introduced natural triols as polyols, such as castor oil. Cramail and coll. reported aqueous PU latexes with 5wt% solid content and particle sizes of 200-300nm²⁴. Sayer and coll. also obtained latexes with 20wt% of solid content with particle sizes of 180 nm and PU molar mass around 5800 g/mol with a dispersity of 1.55.²⁵

In all these examples of PU synthesis through miniemulsion process, the authors pointed out the formation of urea linkages. This is due to the side reaction between water and isocyanate to form amine units that subsequently react with isocyanate to form urea functions. According to Landfester, this side reaction is slower than the reaction of IPDI with alcohol thus limiting the urea content in the final polymer.²²

Furthermore, during the miniemulsion polymerization, a hydrophobic agent is needed to prevent Ostwald ripening. This agent may modify the resulting polymer and the coating features. Hexadecane is the most widely used hydrophobic agent but vegetable oils such as olive oil and açai oil have been tested as hydrophobic agents to prepare polyurethane latexes.²⁴⁻²⁶ To remain on the “green” track, such additives have to be removed. There are scarce examples in the literature of hydrophobe-free miniemulsion polymerization.²⁷⁻²⁹ In all cases, the surfactant is the sole stabilizer and plays also the role of hydrophobe: for Charleux and coll. and Landfester and coll., the surfactant is a comb-like charged copolymer while for Liu and coll., it is a Y-like branched castor oil derivative. More recently, Singha and coll. performed RAFT polymerization of a fluorinated acrylate in miniemulsion. The RAFT agent used contains a long alkyl chain with 12 carbons. The high hydrophobicity of the monomer and the RAFT agent allowed miniemulsion polymerization with SDS or Triton X-450 as surfactant.³⁰

In this study, a hydrophobe-free formulation was developed to get semi-biobased aqueous PU latexes. Sodium dodecyl sulphate (SDS) was used as a surfactant. Two bio-based diols from ricinoleic acid were easily synthesized. The polymerizations were performed in bulk and miniemulsion with solid contents up to 50wt%.

Materials and Method

The biobased diols used in this study are the butanediol monoester **RicBmE** and the propanediol monoester **RicPmE** obtained from ricinoleic acid (**Fig.1**). The synthesis of such diols has already been described by Cramail *et al.*³¹ Isophorone diisocyanate **IPDI** is used as the comonomer and dibutyltin dilaurate (DBTDL) as the catalyst, the latter being used at the concentration of 0.4wt% of the organic phase.

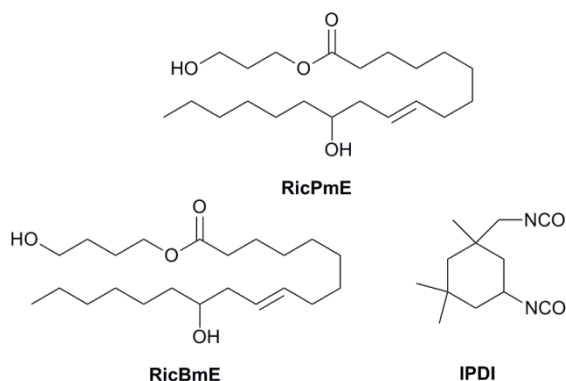


Fig. 1: Castor oil diol derivatives RicBmE, RicPmE and isophorone diisocyanate IPDI.

The organic phase is composed of the monomers, the catalyst and the hydrophobic agent while the aqueous phase consists of deionized water and a surfactant (sodium dodecyl sulphate).

The miniemulsions are obtained by ultrasonication of the system for 120 sec in an ice bath (Bioblock Scientific Vibracell™, 750W, 40% amplitude). Then the polymerization is carried out at 60°C for 4h with mechanical stirring at 300 rpm. Particle sizes were measured by dynamic light scattering (DLS) with a Zetasizer Nano ZS from Malvern. Samples were diluted in continuous phase before analysis.

Results and Discussion

RicBmE and **RicPmE** are easily synthesized in a single step by trans-esterification of ricin oil with 1,4-butanediol or 1,3-propanediol and then polymerized with IPDI catalysed by DBTDL to yield polyurethane. Bulk polymerization of **RicPmE** and IPDI at 60°C leads to an amorphous polymer with a glass transition temperature of 14°C, and Mn of 30 000g/mol ($\bar{D}\approx 3.3$). Similar results are obtained with **RicBmE**.

The system was transposed to miniemulsion. In order to obtain the highest solid content and monomer conversion, parameters such as the solid content, the hydrophobic agent and the number of IPDI equivalent were studied. Finally, the side reaction of isocyanate with water giving urea units was investigated.

Influence of the hydrophobic agent

Two hydrophobic agents were studied: hexadecane and stand oil. The first one is a largely used hydrophobic agent and the second one

is a linseed oil derivative. For 20wt% of solid content, miniemulsions were obtained with similar characteristics whatever the hydrophobic agent. The droplet size of the miniemulsion and the particle size of the latex were similar, around 200nm. The same experiment was performed without hydrophobic agent and similar results were obtained. Results are summarized in **Table 1**.

Surprisingly, no hydrophobic agent was needed to improve the stability of the droplets and the latex particles. This phenomenon is explained by the high hydrophobicity of **RicBmE** molecule^{32,†} which plays the hydrophobe role and thus prevents the Ostwald ripening.

Table 1: Influence of the solid content and the hydrophobic agent on the particle size.

Solid content (wt%)	Hydrophobic agent (3.2wt% of the organic phase)	[SDS] (CMC) ^a	Particle size (nm)[PDI] ^b
20	Hexadecane	3.5	220 [0.206]
20	Stand oil	3.5	210 [0.139]
20	No hydrophobe	3.5	230 [0.180]
30	No hydrophobe	3.5	200 [0.118]
40	No hydrophobe	5.2 ^c	245 [0.176]
50	No hydrophobe	5.2 ^c	270 [0.183]

RicBmE and IPDI were used in stoichiometric proportions. DBTDL concentration was 0.4wt% of the organic phase. ^a 1 CMC= 2.34mg/mL — critical micellar concentration of SDS. ^b Measured by DLS with a 90° angle. ^c Lower amounts of SDS gave unstable miniemulsions.

The solid content can be increased up to 50wt%. Nevertheless, the concentration of SDS in the continuous phase has to be slightly increased for 40 and 50wt% solid content systems to obtain stable systems. When increasing the solid content, the number of particles raises and thus the surface of the interface too. Then, more surfactant is needed to cover the entire surface. Moreover, the particle size increases slightly with the solid content, up to 270nm at 50wt%.

Very interestingly, stable polyurethane latexes could be obtained with solid content up to 50wt% in hydrophobe-free condition.

FTIR analysis of such latexes revealed the presence of urea units in the polymer backbone (see ESI S6). Urea formation during polyurethane synthesis is a known side reaction.²² As the reaction of isocyanates and water leads to the production of amines, and the subsequent reaction of amines with isocyanates to urea, the isocyanate (NCO) concentration is dropping along with the polymerization. Therefore, hydroxyls (OH) are not fully converted at the end of the polymerization.

Hu *et al.* developed a method to calculate the amount of urea and urethane in waterborne PU using ¹H NMR in deuterated DMSO.³³ Protons linked to the nitrogen atom have different chemical shifts in urea and urethane (see **Fig.2.**) enabling to calculate the urea content in the polymers by integration of the corresponding peaks. This method was used to determine the urea content in our systems using **RicPmE** as a diol (see ESI S4, S5). The results are summarized in **Table 2**.

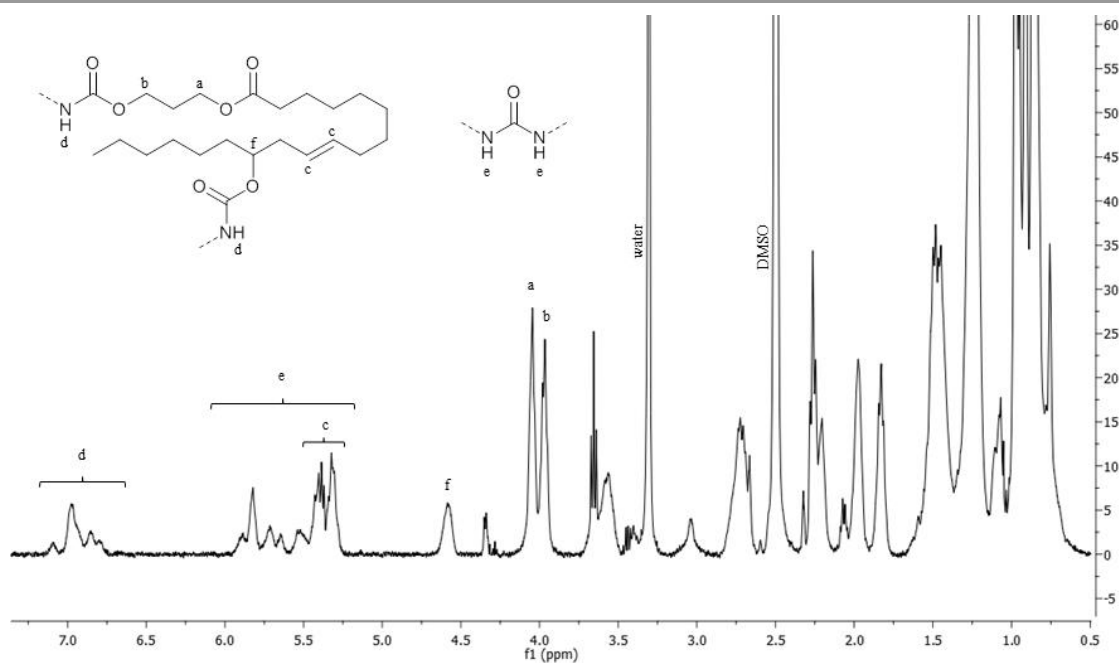


Fig. 2: ^1H NMR in deuterated DMSO of lyophilized polymer latex with partial assignment. (**RicPmE** and IPDI were used as monomers, with 3.5 CMC of SDS. No hydrophobic agent was added. DBTDL concentration was 0.4wt% of the organic phase.)

Table 2: Influence of the hydrophobic agent on the urea content

Solid content (wt%)	Hydrophobic agent (3.2wt% of the organic phase)	Particle size (nm) ^a	Urea content ^b (%)
20	Hexadecane	240±8	24
20	Sunflower oil	250±14	32
20	No hydrophobe	238±19	24

RicPmE and IPDI were used in stoichiometric proportions, with 3.5 CMC of SDS. DBTDL concentration was 0.4wt% of the organic phase.

^a Measured by DLS with a 90° angle. The value given is the average value of three measurements. Polydispersity indexes are between 0.143 and 0.232.

^b Measured from ^1H NMR in DMSO on lyophilized latex.

The results obtained without hydrophobe and with hexadecane are similar with a urea content of 24%. It means that the addition of a hydrophobic agent has no effect on this side reaction. This feature confirms the hypothesis that such side reaction occurs only at the interface of the droplets and that water is not diffusing in the organic phase. Furthermore, the urea content with sunflower oil as hydrophobic agent is higher. Sunflower oil mainly consists of triglycerides (95-99%), but also contains other components such as unsaponifiable derivatives, which could explain the higher urea content.

Influence of the NCO/OH ratio on hydrophobe-free miniemulsion polymerizations

Studies on the influence of the NCO/OH ratio were performed on the system at 20wt% of solid content, with 3.5 CMC of SDS, using **RicPmE** as diol, without hydrophobic agent. The latexes obtained were lyophilized in order to analyse the crude polymers. The same reactions were performed in bulk to compare the polymer characteristics.

Table 3 summarizes the molar mass of the polymers obtained with different NCO/OH ratio both in miniemulsion and bulk polymerization in brackets. In bulk, the molar masses follow the Carothers law: they logically drastically decrease when NCO/OH is

far from the stoichiometry. Obviously, the glass transition temperature follows the same trend.

Table 3: Characteristics of PU latex and [bulk PU]

NCO/OH ratio	Mw ^{a,d} (kg/mol)	Đ ^{a,d}	Particle size ^b (nm)	Tg ^{c,d} (°C)	Urea content ^d (%)
0.8	3.2 [9.6]	1.3 [1.1]	249±11	-16 [-12]	21 [5]
1	3.7 [38.2]	1.4 [3.5]	238±19	-5 [14]	24 [-] ^d
1.2	4.8 [24.5]	1.5 [2.3]	243±7	9 [12]	30 [-] ^d
1.5	5.8 [9.6]	1.6 [1.7]	226±14	32 [-9]	34 [18]
1.8	5.2 [2]	1.5 [1.4]	239±18	69 [-22]	43 [22]
2	4.7 [2]	1.5 [1.4]	228±16	69 [-29]	55 [25]
2.5	4.2	1.4	232±14	nd	55
3	nd	nd	220±6	nd	55

RicPmE and IPDI were used as monomers, with 3.5 CMC of SDS. No hydrophobic agent was added. DBTDL concentration was 0.4wt% of the organic phase. ^a Measured by SEC in THF calibrated with polystyrene standards. ^b Measured by DLS with a 90° angle. The value given is the average value of three measurements. Polydispersity indexes are between 0.162 and 0.234. ^c Measured by differential scanning calorimetry. ^d Polymers insoluble in deuterated DMSO. nd: not determined

Following the mini-emulsion process, the molar masses are lower in comparison to the ones obtained in bulk polymerization and remain practically constant with the NCO/OH ratio. Moreover the particle size is not affected and remains around 240 nm. Indeed, the stoichiometry between the diol and the diisocyanate is difficult to achieve because of the side reaction between isocyanate and water, proved by the presence of unreacted alcohol in the final material. The conversion of each alcohol function (primary and secondary) can be calculated from ^1H NMR spectra in CDCl_3 by integration of the peaks corresponding to the protons in alpha of the hydroxyl

functions (see ESI S7). These hydroxyl functions are those of some **RicPmE** left and of the resulting polymer chain-ends. Results are shown in **Fig.3** for both miniemulsion and bulk polymerisation.

For bulk polymers, as expected, the conversion is complete for both hydroxyl functions when there is enough diisocyanate to reach equivalence.

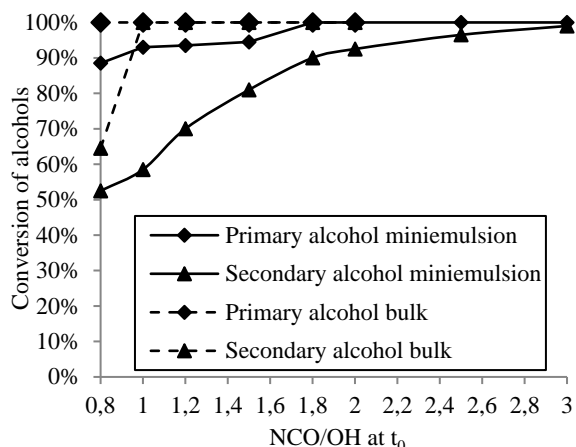


Fig.3: Conversion of primary and secondary alcohols according to ^1H NMR in CDCl_3 . (**RicPmE** and IPDI were used as monomers, with 3.5 CMC of SDS. No hydrophobic agent was added. DBTDL concentration was 0.4wt% of the organic phase.)

For miniemulsion polymers, around the stoichiometric ratio, some unreacted **RicPmE** is left due to the formation of urea. For a NCO/OH ratio of 1.5, there is no more unreacted **RicPmE** but still a lot of secondary OH chain-ends. Thus, by increasing the NCO/OH ratio, one can increase the alcohol conversion without changing the latex particle size and stability. Indeed, full conversion can be achieved with a NCO/OH ratio of 3. In the meantime, the urea content increases thus affecting the polymer properties (**Fig.4**).

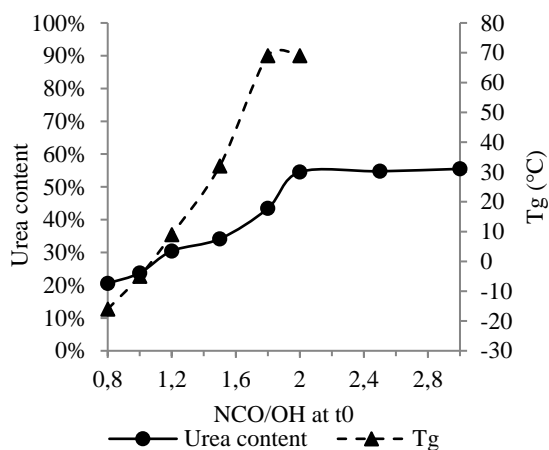


Fig.4: Evolution of the polymer characteristics with the NCO/OH ratio at t_0 for the miniemulsion systems with 3.5 CMC of SDS at 20wt% of solid content. (**RicPmE** and IPDI were used as monomers, with 3.5 CMC of SDS. No hydrophobic agent was added. DBTDL concentration was 0.4wt% of the organic phase.)

The conversion and the urea formation increase with the NCO/OH ratio, from a urea content of 24% to 55% when $\text{NCO/OH} \geq 2$. These poly(urethane-urea)s have different thermomechanical properties

compared to polyurethane. Urea functions harden the polymer, as proved by the higher T_g obtained with the urea content (**Table 3**). These transition temperatures can be compared to the T_g of the bulk polyurethane obtained with $\text{NCO/OH}=1$ which has a T_g of only 12°C (with a negligible quantity of urea). For NCO/OH ratios of 0.8 to 1.2, the T_g is below 12°C , explained by the presence of unreacted **RicPmE** (**Fig.3**) that plasticises the polymer and thus decreases the T_g .

Finally, full diol conversion can be reached by playing with the NCO/OH ratio, and the polyurethane-urea thermomechanical properties can be modulated.

Conclusions

High solid content bio-based poly(urethane-urea) latexes were obtained through miniemulsion polymerization. No hydrophobic agent was needed. The hydrophobic vegetable-based diol itself allows stabilizing the droplets against Ostwald ripening. Thus, the use of solvents or additives is avoided during the whole polymerization process. Lower molar masses compared to the bulk polymerization were observed, however the thermomechanical properties of these polymers can be modulated using different monomer ratios.

Notes and references

^a Centre National de la Recherche Scientifique, Laboratoire de Chimie des Polymères Organiques, UMR 5629, F-33607 Pessac Cedex, France.

^b Université de Bordeaux, Laboratoire de Chimie des Polymères Organiques, UMR 5629, F-33607 Pessac Cedex, France

^c ITERG, 11 rue Gaspard Monge, Parc Industriel, Pessac Cedex, F-33600, France

† LogP and logS can be calculated using ALOGPS 2.1 software online: VCCLAB, Virtual Computational Chemistry Laboratory, <http://www.vcclab.org>, 2005 (accessed in March 2013). The logP and logS values of RicBmE are lower than hexadecane but in the same range as decane: $\log P=6.13$ and $\log S=-5.34$.

- M. Muro-Small and D. Neckers, *ACS Sustain. Chem. Eng.*, 2013, **1**, 1214–1217.
- U. Biermann, U. Bornscheuer, M. A. R. Meier, J. O. Metzger, and H. J. Schäfer, *Angew. Chemie Int. Ed.*, 2011, **50**, 3854–3871.
- C. Vilela, A. F. Sousa, A. C. Fonseca, A. C. Serra, J. F. J. Coelho, C. S. R. Freire, and A. J. D. Silvestre, *Polym. Chem.*, 2014, **5**, 3119–3141.
- J. O. Metzger, *Eur. J. Lipid Sci. Technol.*, 2009, **111**, 865–876.
- Y. Xia and R. C. Larock, *Green Chem.*, 2010, **12**, 1893–1909.
- L. Maisonneuve, T. Lebarbé, E. Grau, and H. Cramail, *Polym. Chem.*, 2013, **4**, 5472–5517.
- M. Desroches, M. Escouvois, R. Auvergne, S. Caillol, and B. Boutevin, *Polym. Rev.*, 2012, **52**, 38–79.
- E. Del Rio, G. Lligadas, J. C. Ronda, M. Galià, M. A. R. Meier, and V. Cádiz, *J. Polym. Sci. Part A Polym. Chem.*, 2011, **49**, 518–525.
- Z. S. Petrović, D. Hong, I. Javni, N. Erina, Z. Fan, J. Ilavský, and F. Zhang, *Polymer*, 2013, **54**, 372–380.
- M. F. Sonnenschein, V. V. Ginzburg, K. S. Schiller, and B. L. Wendt, *Polymer*, 2013, **54**, 1350–1360.
- K. I. Suresh, *ACS Sustain. Chem. Eng.*, 2013, **1**, 232–242.
- A. More, L. Maisonneuve, T. Lebarbé, B. Gadenne, C. Alfios, and H. Cramail, *Eur. J. Lipid Sci. Technol.*, 2013, **115**, 61–75.
- A. More, T. Lebarbé, and L. Maisonneuve, *Eur. Polym. J.*, 2013, **49**, 823–833.
- C. Fu, Z. Zheng, Z. Yang, Y. Chen, and L. Shen, *Prog. Org. Coatings*, 2013, **77**, 53–60.

15. L. Raghunanan, J. Yue, and S. Narine, *J. Am. Oil Chem. Soc.*, 2013, 1–8.
16. D. Dieterich, *Prog. Org. Coatings*, 1981, **9**, 281–340.
17. T. F. Garrison, M. R. Kessler, and R. C. Larock, *Polymer*, 2014, **55**, 1004–1011.
18. J. Bullermann, S. Friebe, T. Salthammer, and R. Spohnholz, *Prog. Org. Coatings*, 2013, **76**, 609–615.
19. Y. Li, A. J. Noordover, R. A. T. M. van Benthem, and C. E. Koning, *Eur. Polym. J.*, 2014, **52**, 12–22.
20. Y. Li, B. A. J. Noordover, R. A. T. M. van Benthem, and C. E. Koning, *ACS Sustain. Chem. Eng.*, 2014, **2**, 788–797.
21. K. Landfester, F. Tiarks, H.-P. Hentze, and M. Antonietti, *Macromol. Chem. Phys.*, 2000, **201**, 1–5.
22. F. Tiarks, K. Landfester, and M. Antonietti, *J. Polym. Sci. Part A Polym. Chem.*, 2001, **39**, 2520–2524.
23. C.-Y. Li, Y.-H. Li, K.-H. Hsieh, and W.-Y. Chiu, *J. Appl. Polym. Sci.*, 2008, **107**, 840–845.
24. B. G. Zanetti-Ramos, E. Lemos-Senna, V. Soldi, R. Borsali, E. Cloutet, and H. Cramail, *Polymer*, 2006, **47**, 8080–8087.
25. A. Valério, S. R. P. da Rocha, P. H. H. Araújo, and C. Sayer, *Eur. J. Lipid Sci. Technol.*, 2014, **116**, 24–30.
26. B. G. Zanetti-Ramos, E. Lemos-Senna, H. Cramail, E. Cloutet, R. Borsali, and V. Soldi, *Mater. Sci. Eng. C*, 2008, **28**, 526–531.
27. Z. Qian, J. Chen, Y. Chen, Z. Zhang, and H. Liu, *Colloids Surfaces A Physicochem. Eng. Asp.*, 2007, **295**, 7–15.
28. M. Manguian, M. Save, C. Chassenieux, and B. Charleux, *Colloid Polym. Sci.*, 2005, **284**, 142–150.
29. G. Baskar, K. Landfester, and M. Antonietti, *Macromolecules*, 2000, **33**, 9228–9232.
30. A. Chakrabarty and N. K. Singha, *J. Colloid Interface Sci.*, 2013, **408**, 66–74.
31. D. V. Palaskar, A. Boyer, E. Cloutet, J.-F. Le Meins, B. Gadenne, C. Alfos, C. Farcet, and H. Cramail, *J. Polym. Sci. Part A Polym. Chem.*, 2012, **50**, 1766–1782.
32. I. V. Tetko, J. Gasteiger, R. Todeschini, A. Mauri, D. Livingstone, P. Ertl, V. a Palyulin, E. V. Radchenko, N. S. Zefirov, A. S. Makarenko, V. Y. Tanchuk, and V. V. Prokopenko, *J. Comput. Aided. Mol. Des.*, 2005, **19**, 453–63.
33. S. Zhang, L. Cheng, and J. Hu, *J. Appl. Polym. Sci.*, 2003, **90**, 257–260.

Electronic Supporting information:

Hydrophobe-free miniemulsion polymerization: towards high solid content of fatty acid-based poly(urethane-urea)s latexes

E. Rix,^{ab} G. Ceglia,^{ab} J. Bajt,^{ab} G. Chollet,^c V. Heroguez,^{ab} E. Grau^{ab} and H. Cramail^{*ab}

Contents

S1: Polymerization protocols	2
S2: Experimental data	3
S3: ¹ H NMR of RicBmE and RicPmE in CDCl ₃	4
S4: Method to calculate the urea content	5
S5: NMR spectra of lyophilized latex and bulk polymers in DMSO	8
S6: FTIR spectra of lyophilized latex	10
S7: ¹ H NMR of lyophilized latex and bulk polymers in CDCl ₃	11
S8: SEC graphs of lyophilized latex and bulk polymers.....	13
S9: DSC Thermograms	26

S1: Polymerization protocols

Bulk polymerization:

Both monomers and the catalyst are introduced in a tubular schlenk. The polymerization is performed at 60°C under magnetic stirring for 4h. The stirring is no more efficient when the viscosity of the mixture increases. Then the oil bath is removed and samples are taken for analysis.

Miniemulsion polymerization:

Preparation of the aqueous phase:

Sodium dodecyl sulfate is dissolved in deionized water under magnetic stirring until complete dissolution.

Preparation of the organic phase and emulsification:

Both monomers and the catalyst are stirred manually with a spatula for about 10s. The organic phase is then introduced in the aqueous phase previously prepared. Sonication is applied to the system. During sonication, an ice bath is used to cool the system. An emulsion is obtained.

Polymerization:

Shortly after emulsification, the emulsion is inserted in a round-bottom flask equipped with a mechanic stirrer at 60°C. Polymerization is performed for 4h at this temperature with a stirring of 300rpm.

S2: Experimental data

^1H and ^{13}C -NMR spectra were recorded on Bruker Avance 400 spectrometer.

Size exclusion chromatography (SEC) analyses were performed in THF (40°C) on a PL-GPC 50 plus Integrated GPC from Polymer laboratories-Varian with a series of four columns from TOSOH (TSKgel TOSOH: HXL-L (guard column 6,0mm ID x 4,0cm L); G4000HXL (7,8mm ID x 30,0cm L) ;G3000HXL (7,8mm ID x 30,0cm L) and G2000HXL (7,8mm ID x 30,0cm L)). The elution of the filtered samples was monitored using simultaneous refractive index and UV detection. The elution times were converted to molar mass using a calibration curve based on low dispersity (M_w/M_n) polystyrene (PS) standards.

Differential scanning calorimetry (DSC) thermograms were measured using a DSC Q100 apparatus from TA instruments. For each sample, two cycles from -50 to 100 °C (or 120 °C for higher melting point polyurethanes) at 10 °C.min⁻¹ were performed and then the glass transition temperatures were calculated from the second heating run.

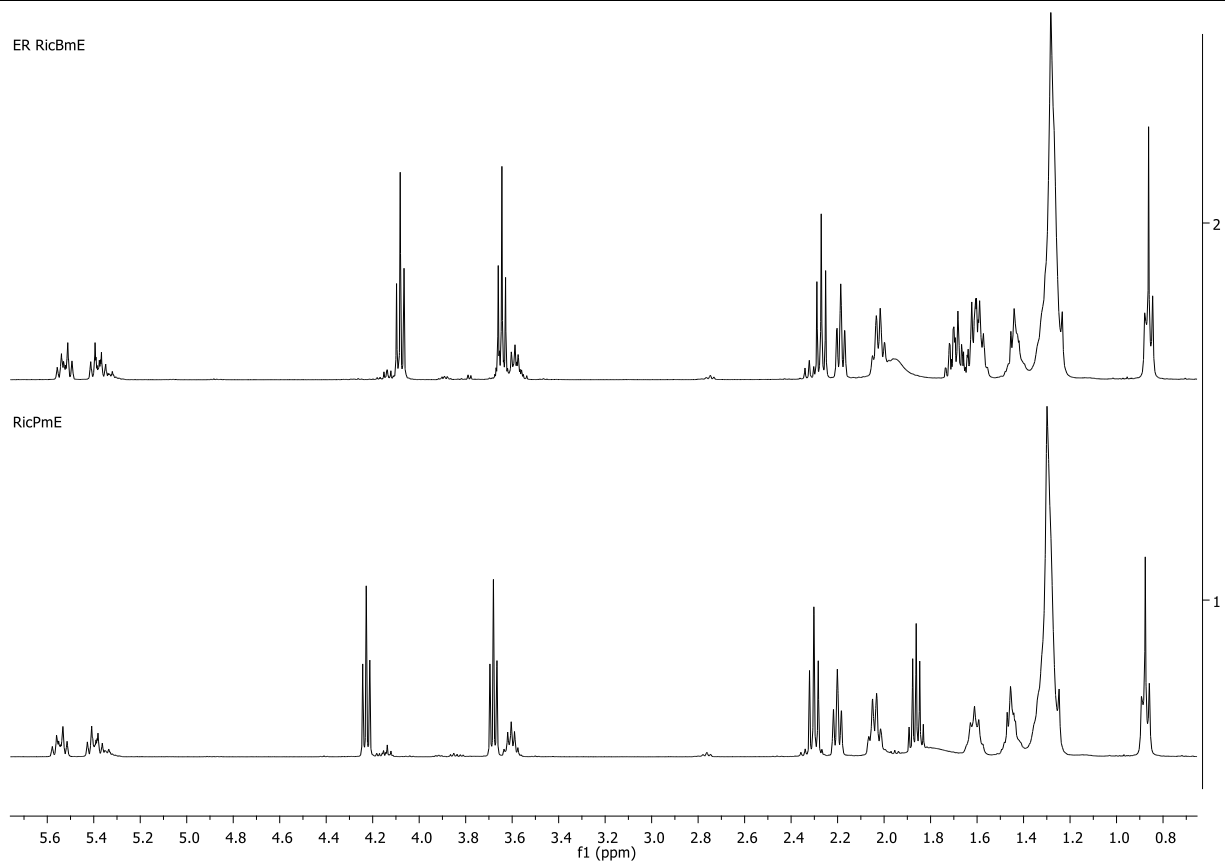
Table 1: Characteristics of PU latex and [bulk PU]

Entry	NCO/OH ratio	M_w ^{a,d} (kg/mol)	\bar{D} ^{a,d}	Particle size ^b (nm)	Tg ^{c,d} (°C)	Urea content ^d (%)
ME0[YP40]	0.8	3.2 [9.6]	1.3 [1.1]	249±11	-16 [-12]	21 [5]
ME1[YP41]	1	3.7 [38.2]	1.4 [3.5]	238±19	-5 [14]	24 [-] ^e
ME2[YP42]	1.2	4.8 [24.5]	1.5 [2.3]	243±7	9 [12]	30 [-] ^e
ME3[YP43]	1.5	5.8 [9.6]	1.6 [1.7]	226±14	32 [-9]	34 [18]
ME4[YP44]	1.8	5.2 [2]	1.5 [1.4]	239±18	69 [-22]	43 [22]
ME5[YP45]	2	4.7 [2]	1.5 [1.4]	228±16	69 [-29]	55 [25]
ME8	2.5	4.2	1.4	232±14	<i>nd</i>	55
ME9	3	<i>nd</i>	<i>nd</i>	220±6	<i>nd</i>	55

RicPmE and IPDI were used as monomers, with 3.5 CMC of SDS. No hydrophobic agent was added. DBTDL concentration was 0.4wt% of the organic phase

^a Measured by SEC in THF calibrated with polystyrene standards. ^b Measured by DLS with a 90° angle. The value given is the average value of three measurements. Polydispersity indexes are between 0.162 and 0.234. ^c Measured by differential scanning calorimetry. ^d Polymers insoluble in deuterated DMSO. *nd*: not determined

S3: ^1H NMR of RicBmE and RicPmE in CDCl_3



S4: Method to calculate the urea content

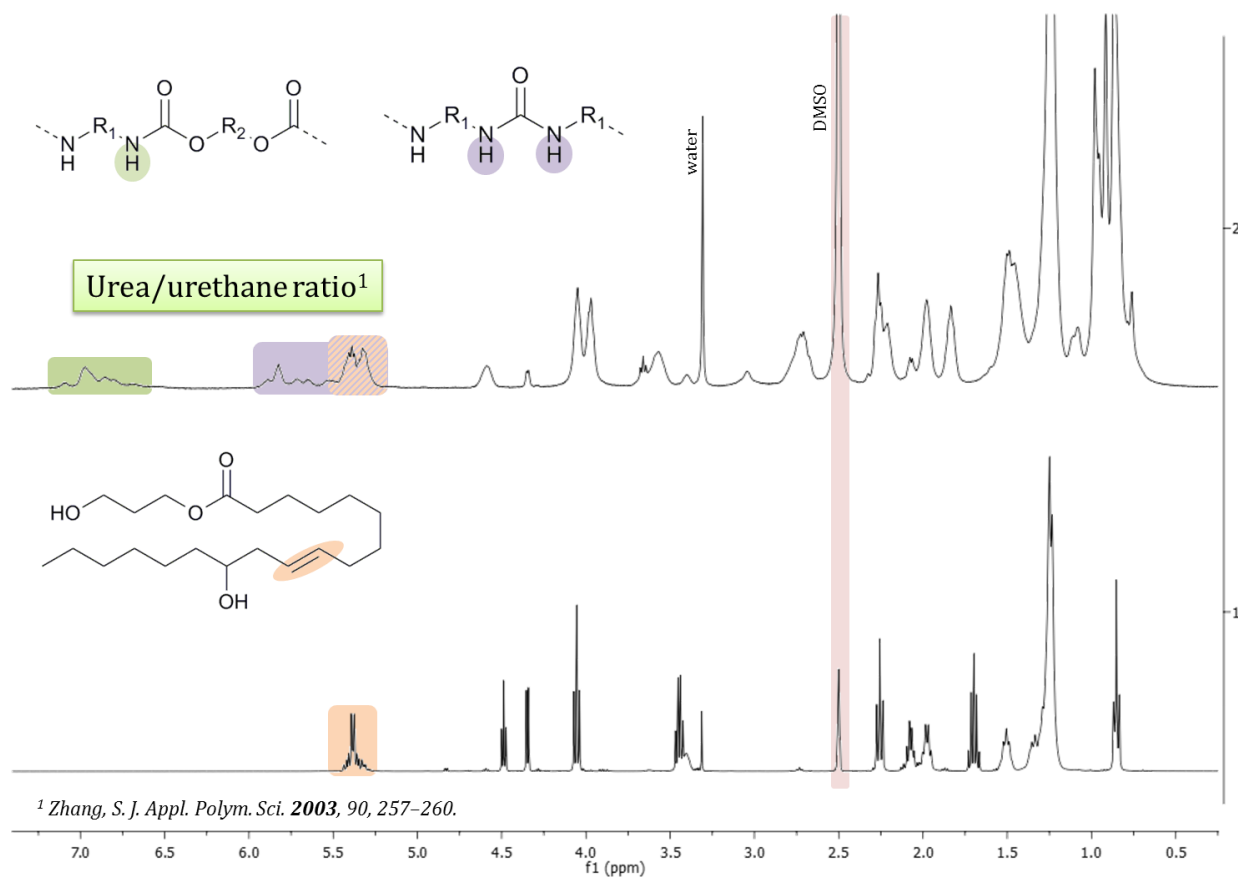


Figure 1: NMR Spectra in DMSO of a lyophilized latex and of RicPmE

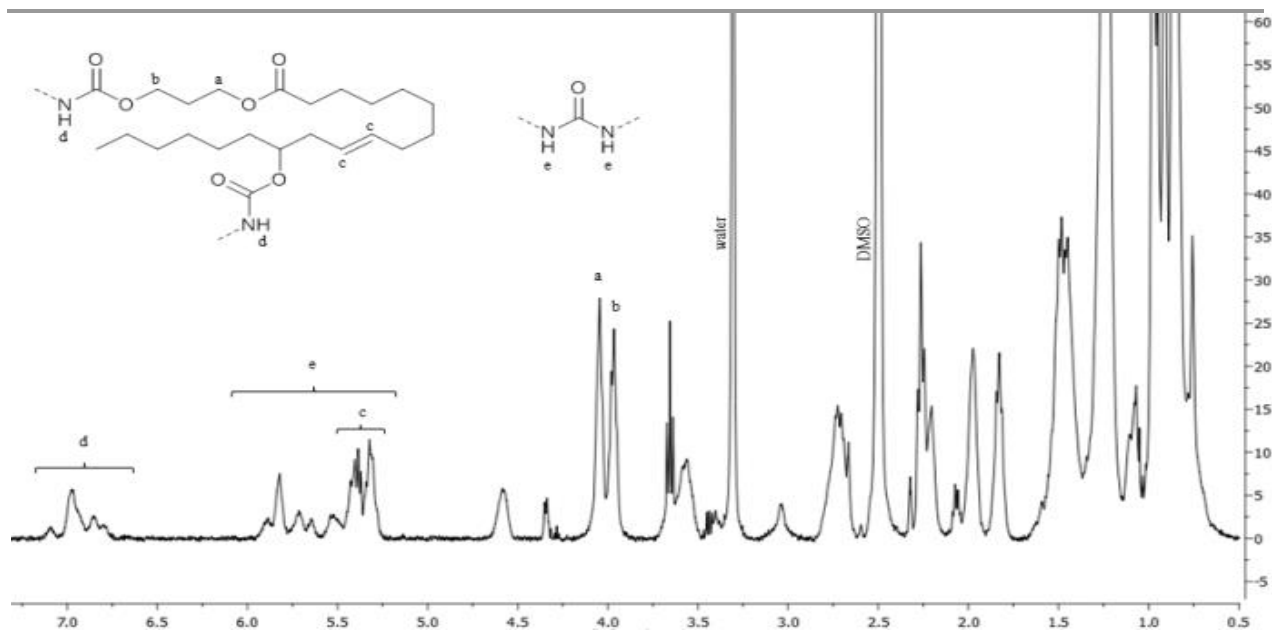


Figure 2: NMR Spectra in DMSO of a lyophilized latex

$$\text{Urea content} = \frac{\text{urea}}{\text{urea} + \text{urethane}}$$

Where:

- $\text{urethane} = d$
- $\text{urea} = \frac{(c+e)-(a+b+2f)/2}{2}$

Equation 1: Definition of the urea content

a, b, c, d, e and f are the integrals corresponding to the following peaks: . f is the integral of the peak at 4.49ppm corresponding to the proton of the unreacted primary alcohol of RicPmE. f=0 when there is no more unreacted primary alcohol.
a + b is set to 4, as it corresponds to 4 protons.

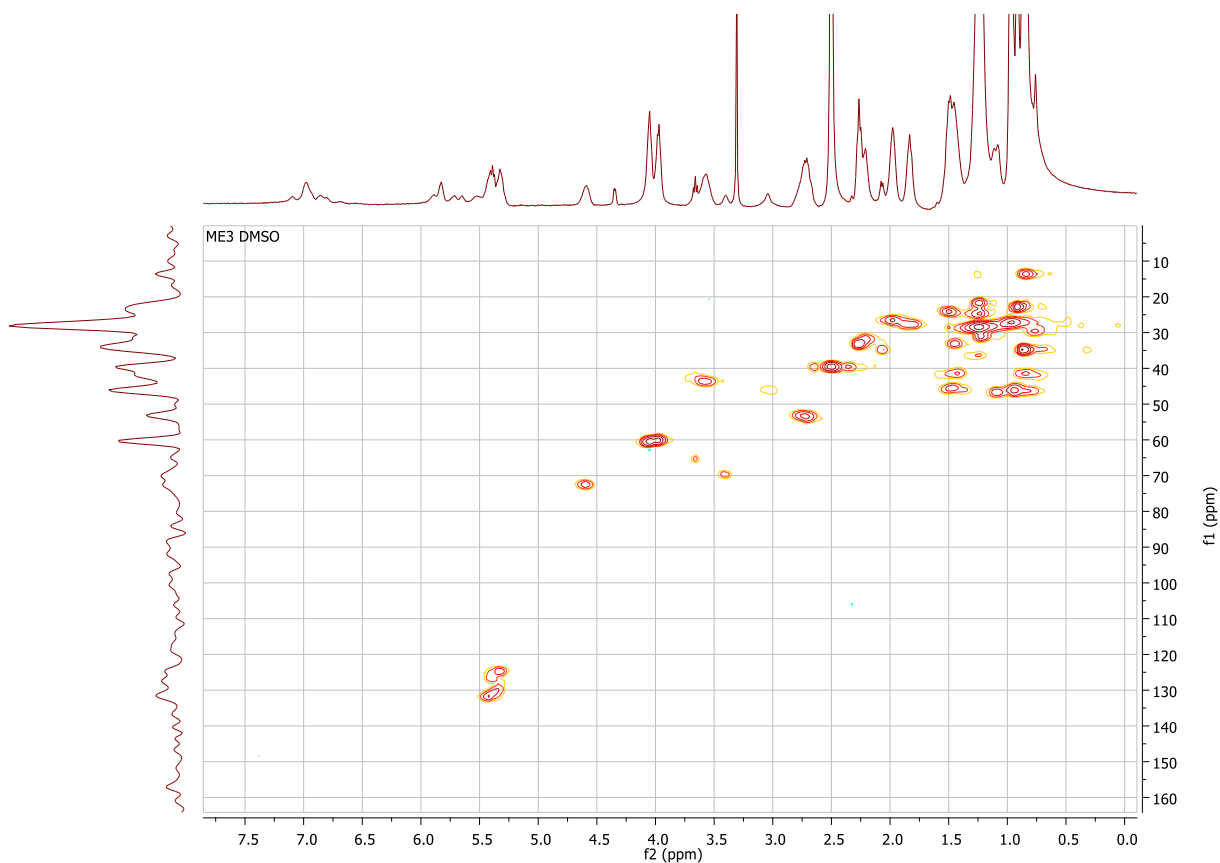


Figure 3: ^{13}C - ^1H NMR of a lyophilized latex in DMSO.

It shows that the protons between 5 and 7.5ppm are not linked to a carbon atom. Only the protons of the double bond are visible in this range

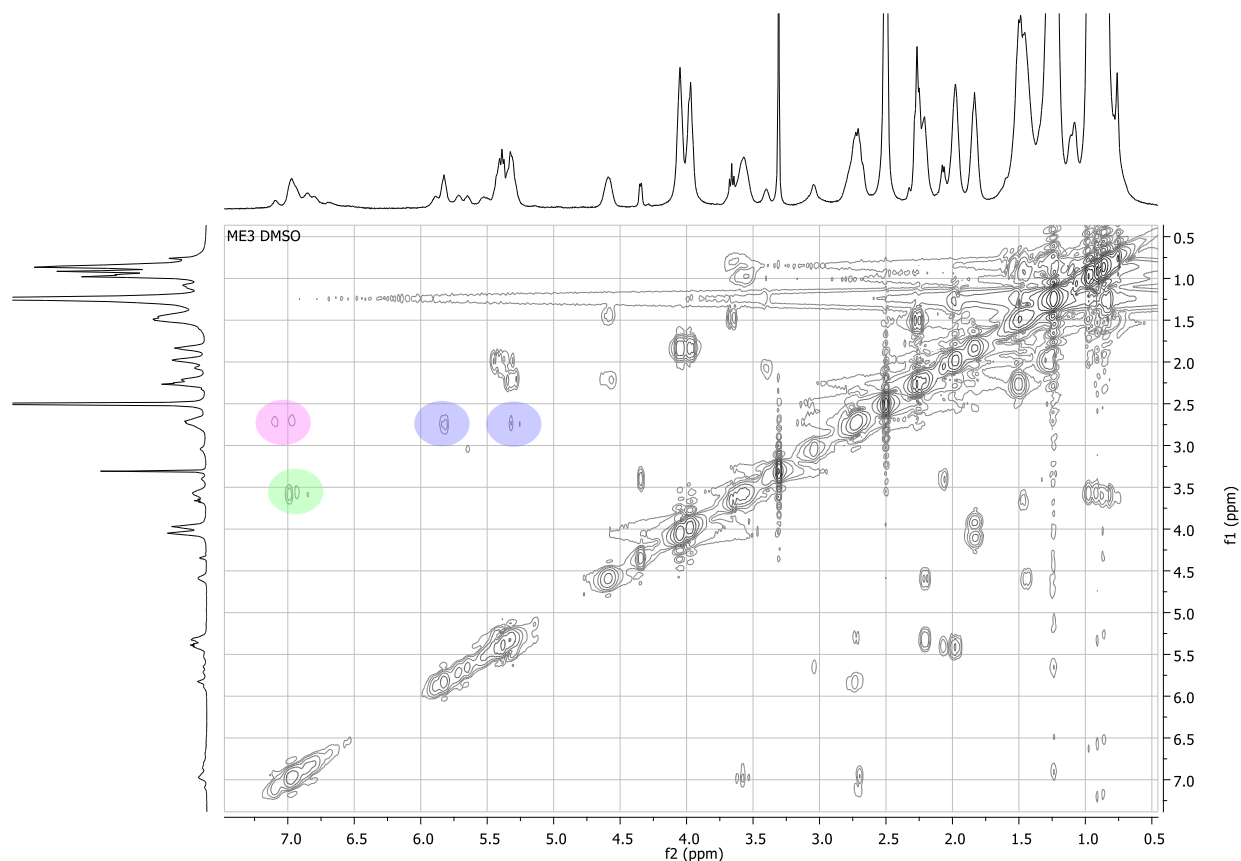
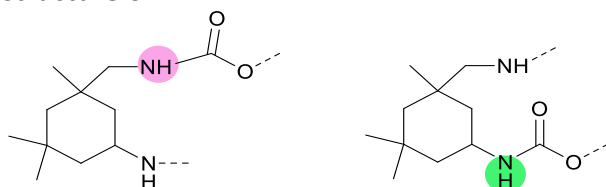
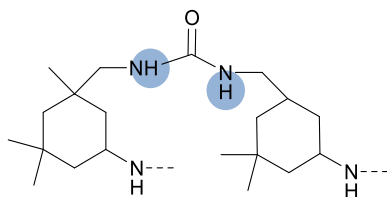


Figure 4: 1H-1H NMR spectrum in DMSO of a lyophilized latex

Around 7ppm (X axis), two correlation signals appear (in pink and green): they correspond to the proton of the NH of urethane functions. There are two signals because of the asymmetrical structure of IPDI.



Between 5 and 6ppm (X axis), signals corresponding to the double bond protons are visible. Two signals are visible (in blue), they correspond to the urea formed with the structure below.



Two other urea structures could be formed, but they are not visible on the NMR spectra. This can be explained by the different reactivity of the two isocyanate functions of the IPDI due to steric hindrance. The more reactive functions react with alcohols, then the less reactive with the alcohol functions remaining. Thus, when the side reaction of isocyanate and water occurs, the less reactive isocyanate function is the main one remaining.

S5: NMR spectra of lyophilized latex and bulk polymers in DMSO

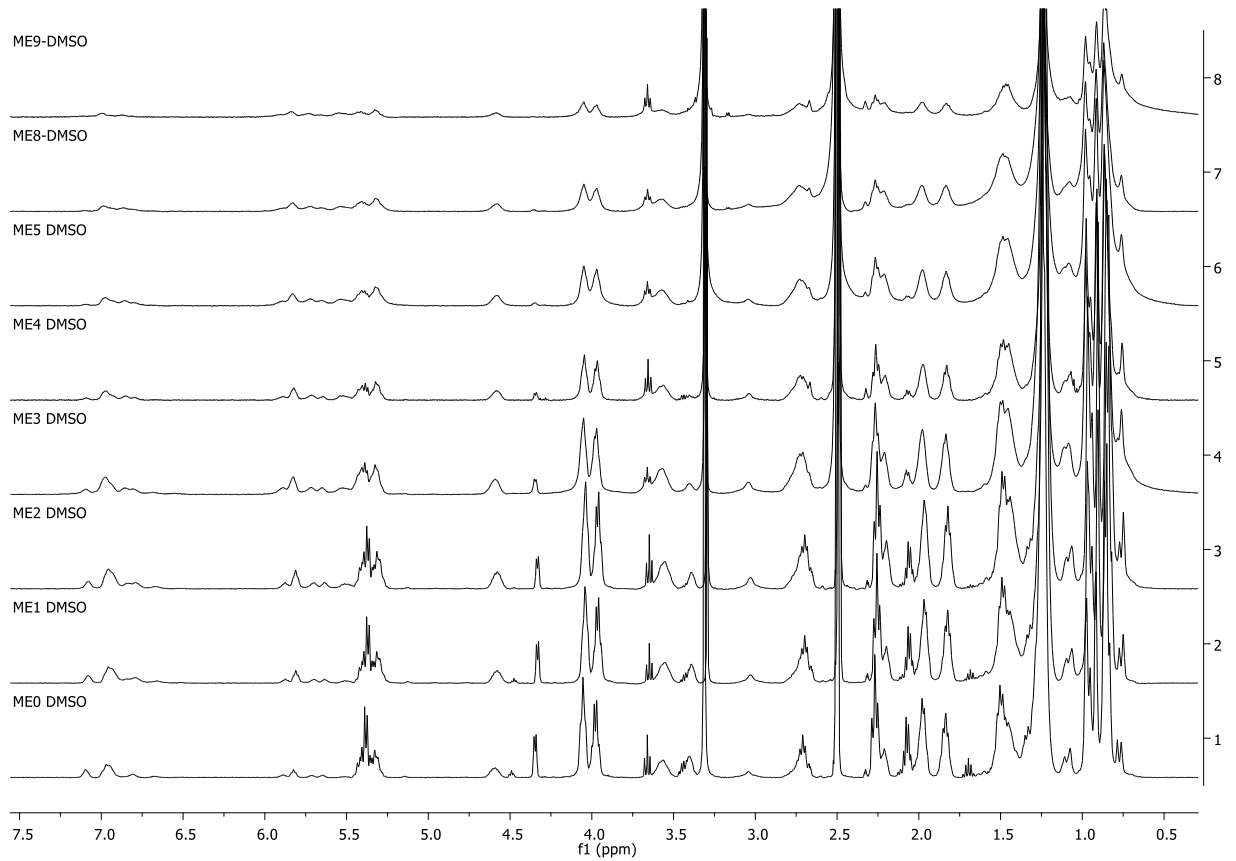


Figure 2: NMR spectra of lyophilized latex ME0 to ME9 in DMSO

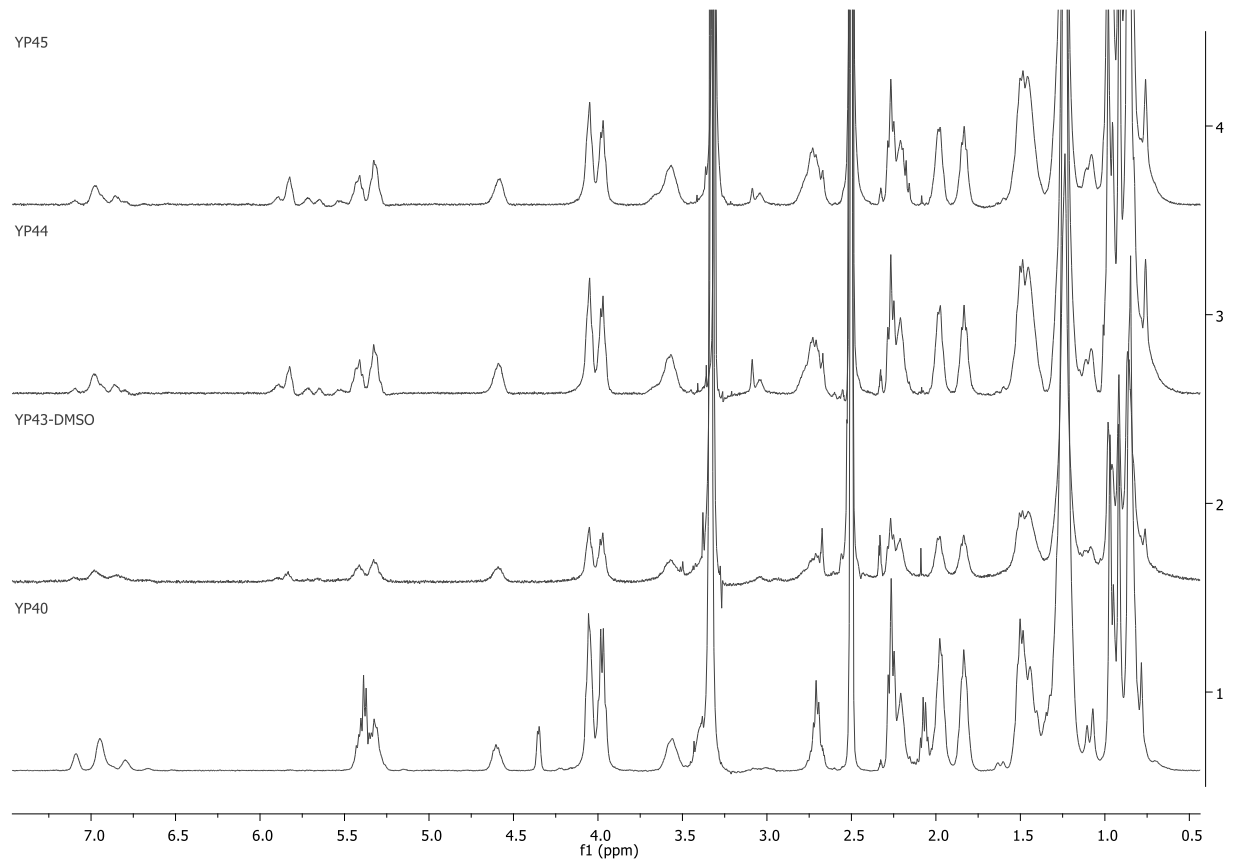
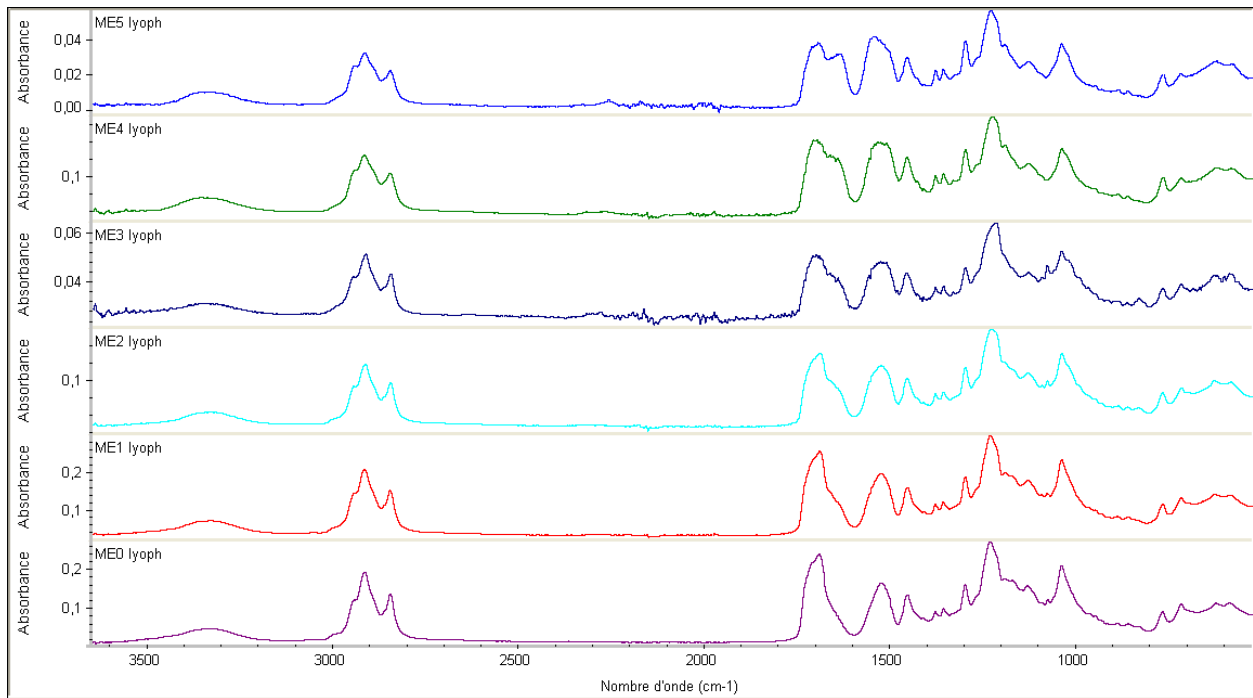


Figure 3: NMR spectra of bulk polymers in DMSO

S6: FTIR spectra of lyophilized latex



The peak at 1645cm⁻¹ is due to the carbonyl group of urea. The peak at 1700cm⁻¹ is due to the carbonyl group of urea. Urea increases with the amount of IPDI introduced which is in accordance with the urea contents calculated from ¹H NMR.

S7: ^1H NMR of lyophilized latex and bulk polymers in CDCl_3

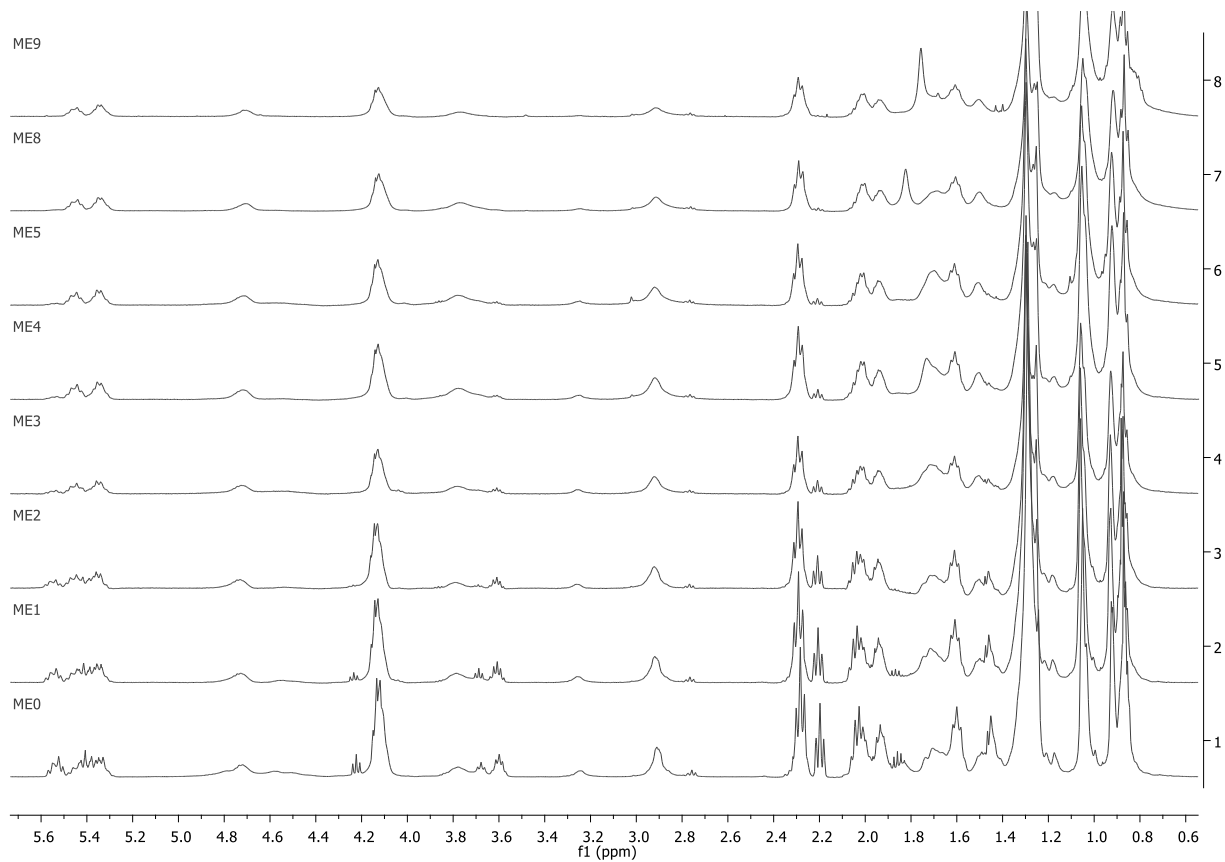


Figure 4: NMR spectra of lyophilized latex ME0 to ME9 in CDCl_3

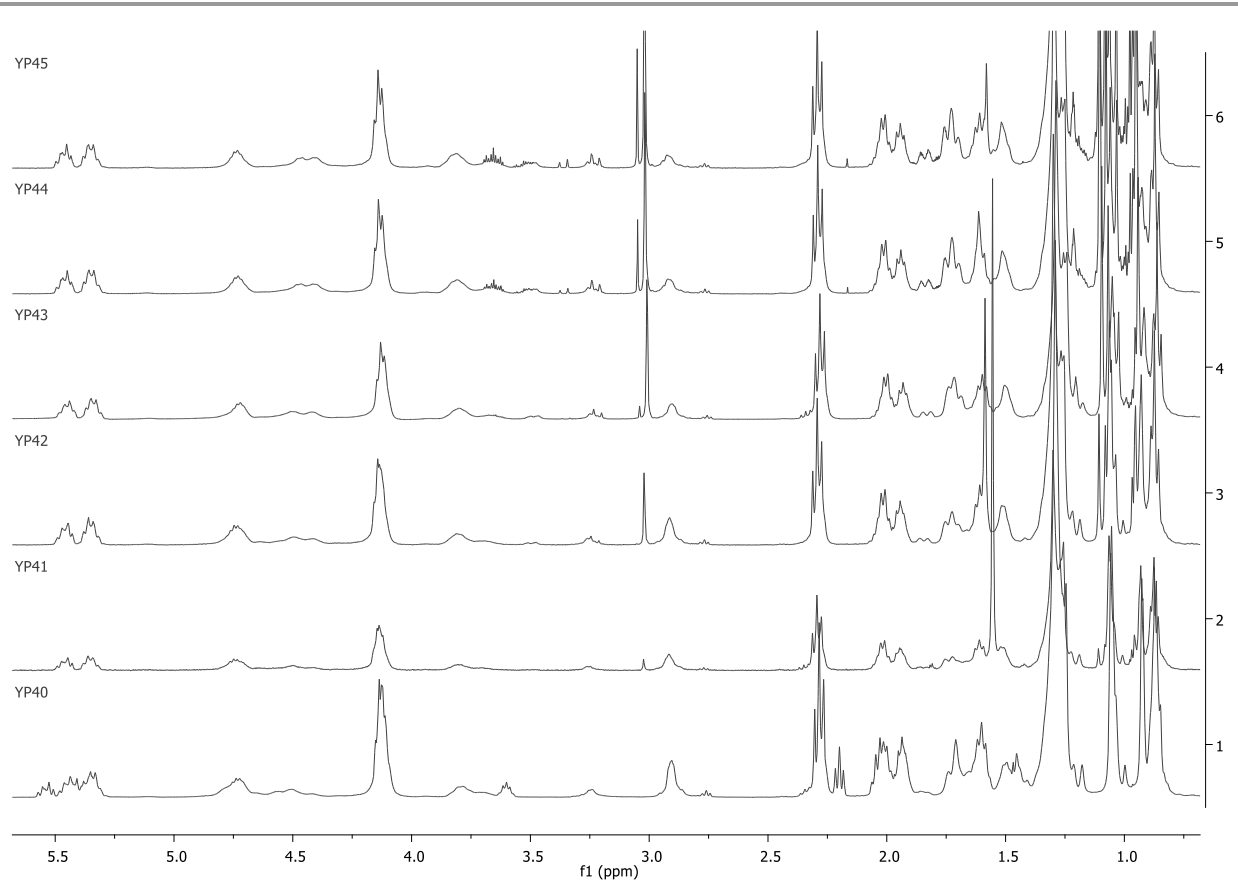
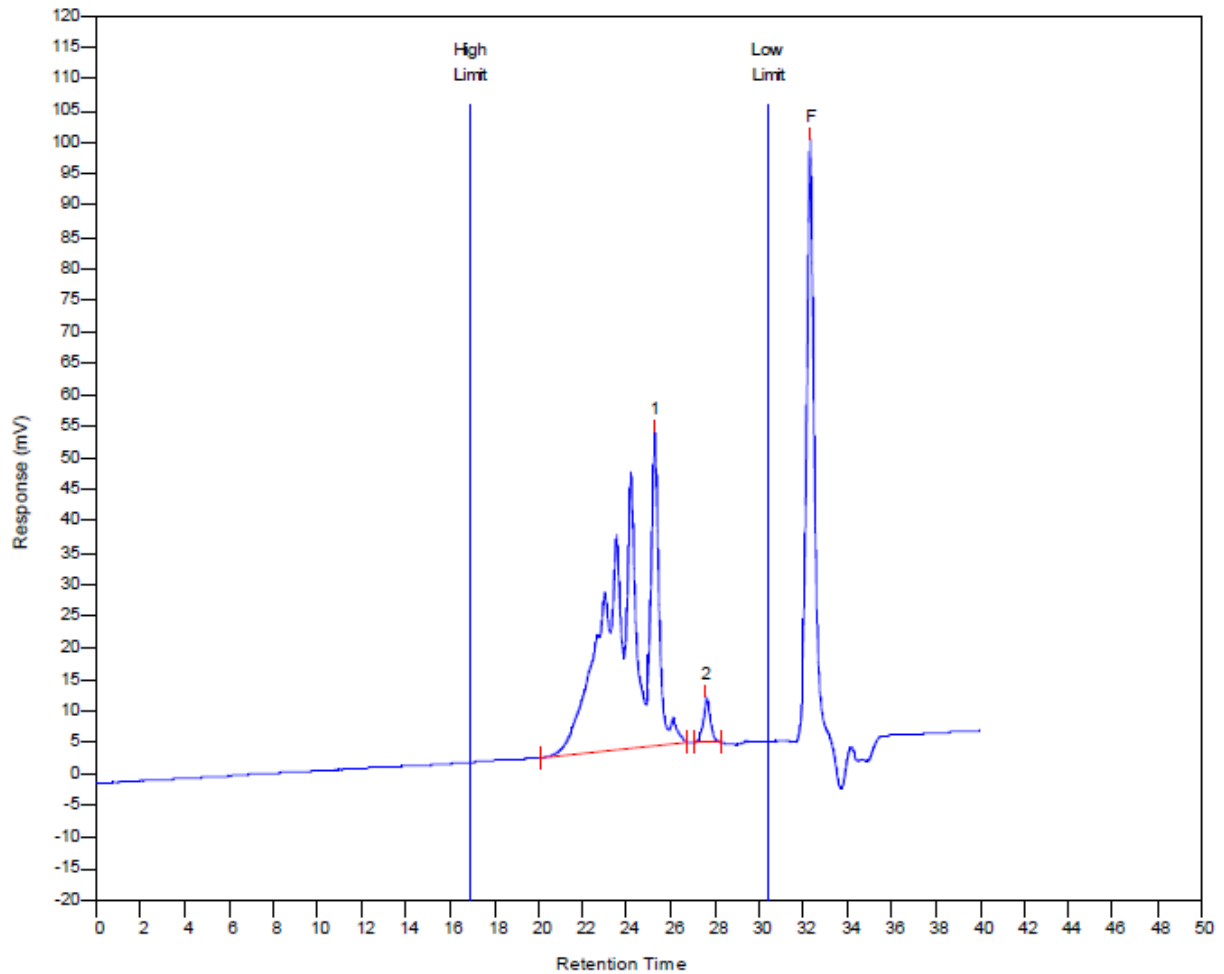


Figure 5: NMR spectra of bulk polymers in CDCl₃

S8: SEC graphs of lyophilized latex and bulk polymers

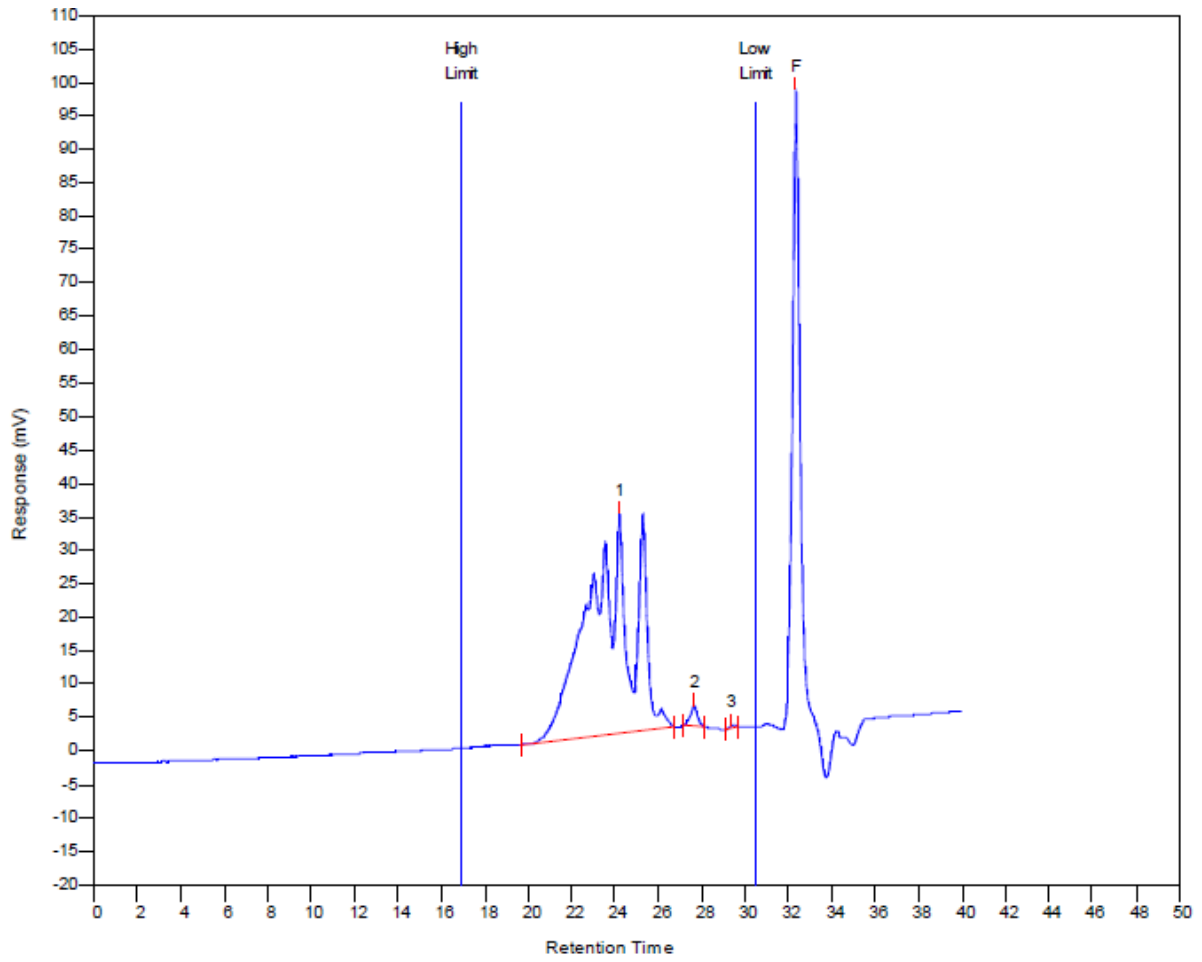
ME0



MW Averages

Peak No	Mp	Mn	Mw	Mz	Mz+1	Mv	PD
1	1491	2406	3166	4282	5674	3027	1.31588
2	583	580	583	586	589	582	1.00517
3	0	0	0	0	0	0	0

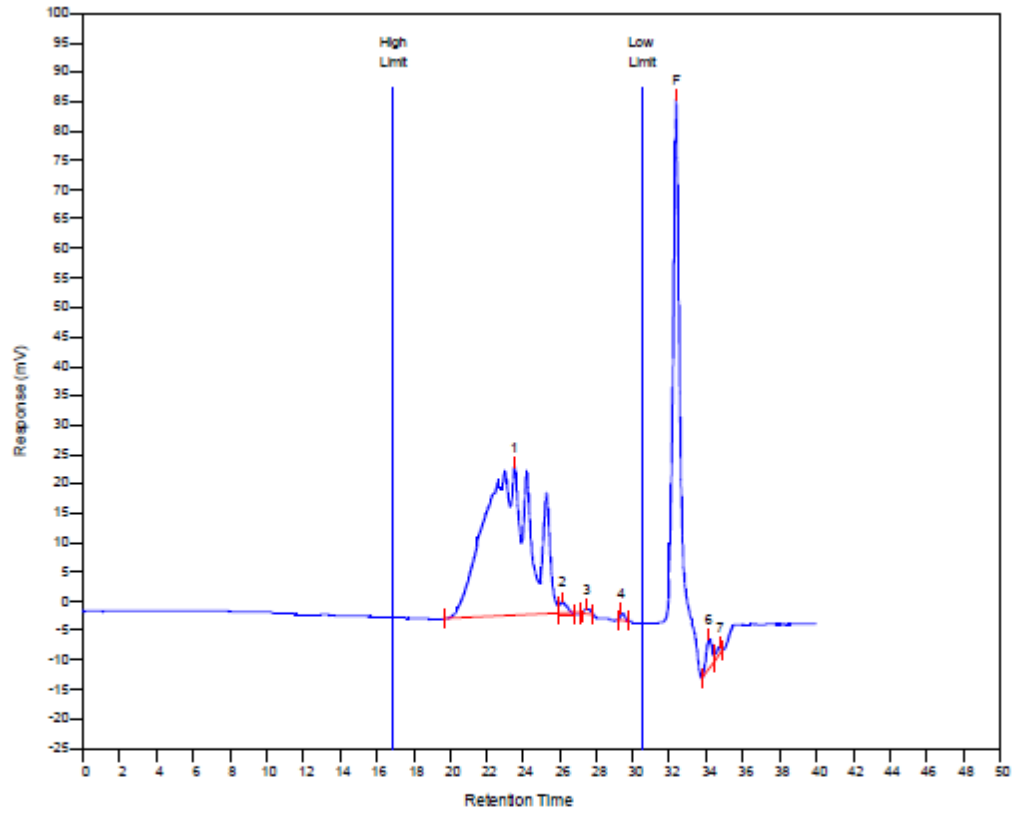
ME1



MW Averages

Peak No	Mp	Mn	Mw	Mz	Mz+1	Mv	PD
1	2345	2681	3685	5136	6893	3503	1.37449
2	582	588	590	593	595	590	1.0034
3	271	273	272	273	274	271	0.996337
4	46	44	45	46	47	45	1.02273

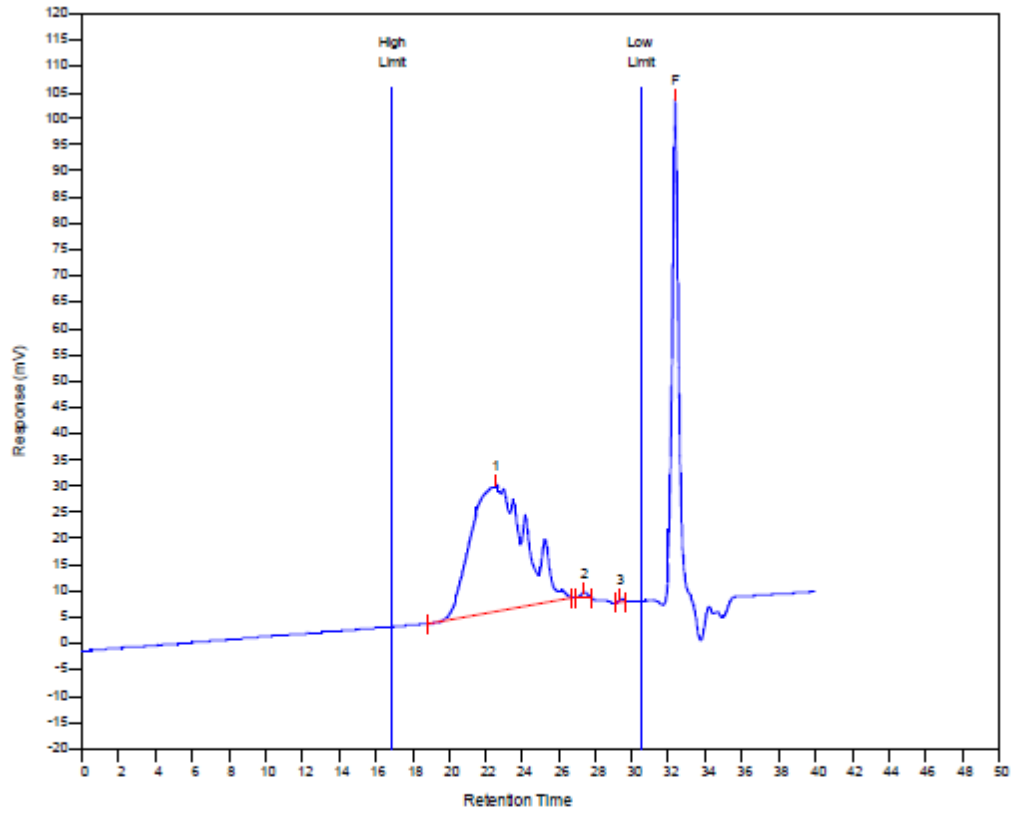
ME2



MW Averages

Peak No	Mp	Mn	Mw	Mz	Mz+1	Mv	PD
1	3201	3296	4786	6973	9596	4513	1.45206
2	1082	1067	1003	1044	1050	988	0.940019
3	594	617	617	620	622	616	1
4	269	268	268	269	270	268	1

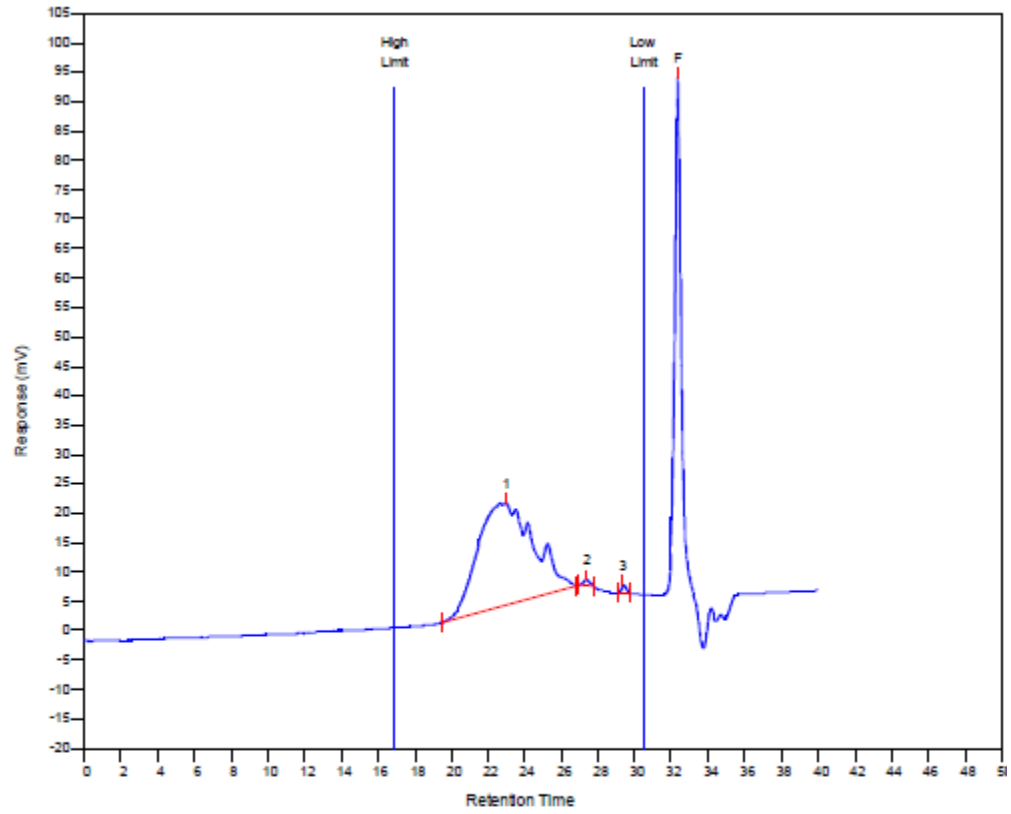
ME3



MW Averages

Peak No	Mp	Mn	Mw	Mz	Mz+1	Mv	PD
1	4993	3759	5845	8683	11827	5480	1.55493
2	645	652	654	658	661	653	1.00307
3	269	269	269	270	271	268	1

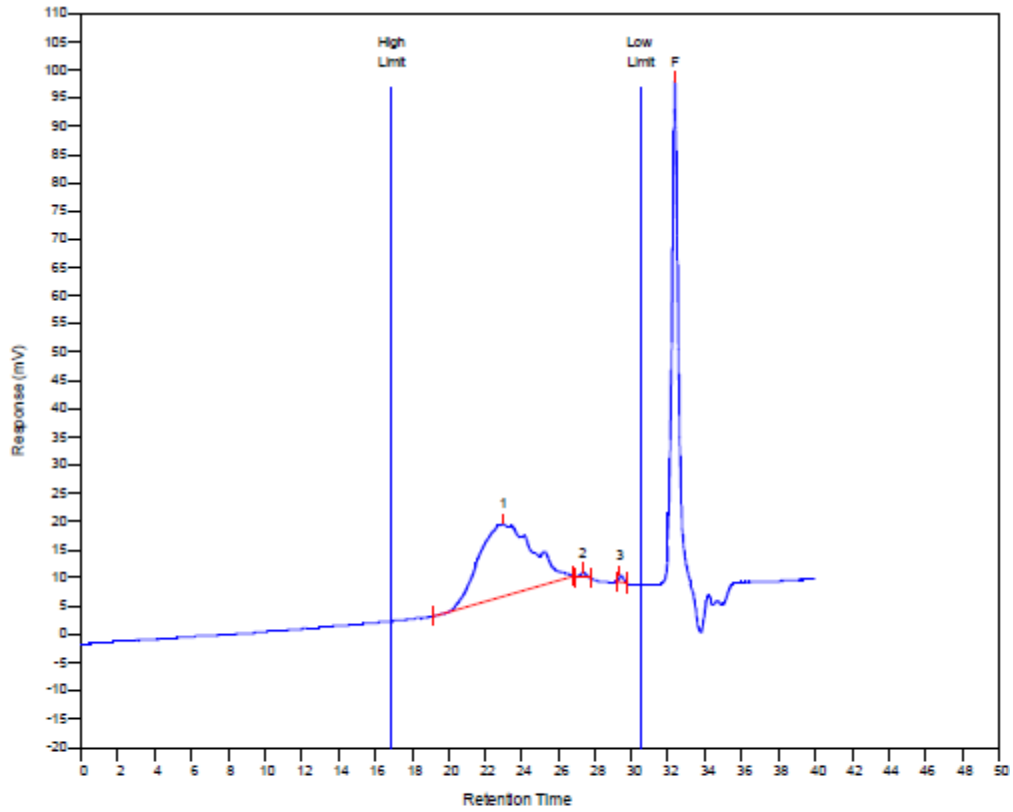
ME4



MW Averages

Peak No	Mp	Mn	Mw	Mz	Mz+1	Mv	PD
1	4993	3415	5183	7654	10539	4870	1.51772
2	649	660	661	665	668	660	1.00152
3	269	268	268	269	270	268	1

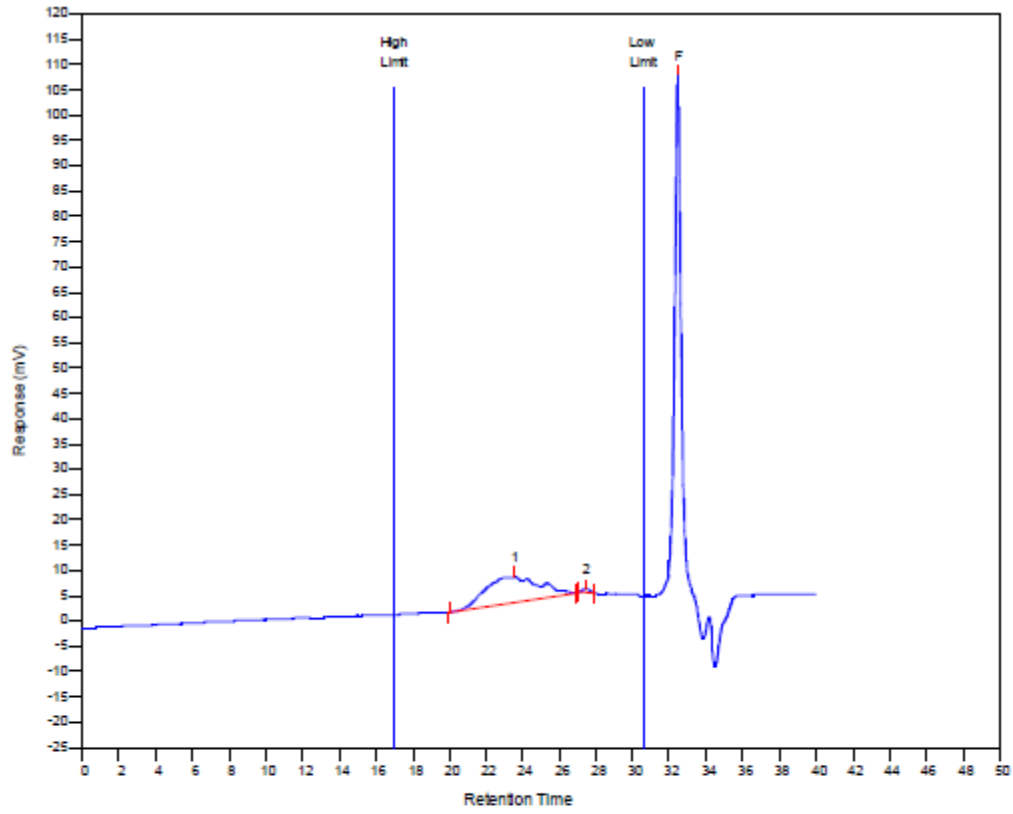
ME5



MW Averages

Peak No	Mp	Mn	Mw	Mz	Mz+1	Mv	PD
1	4155	3192	4692	6762	9155	4429	1.46992
2	662	657	658	662	664	657	1.00152
3	269	267	267	268	269	267	1

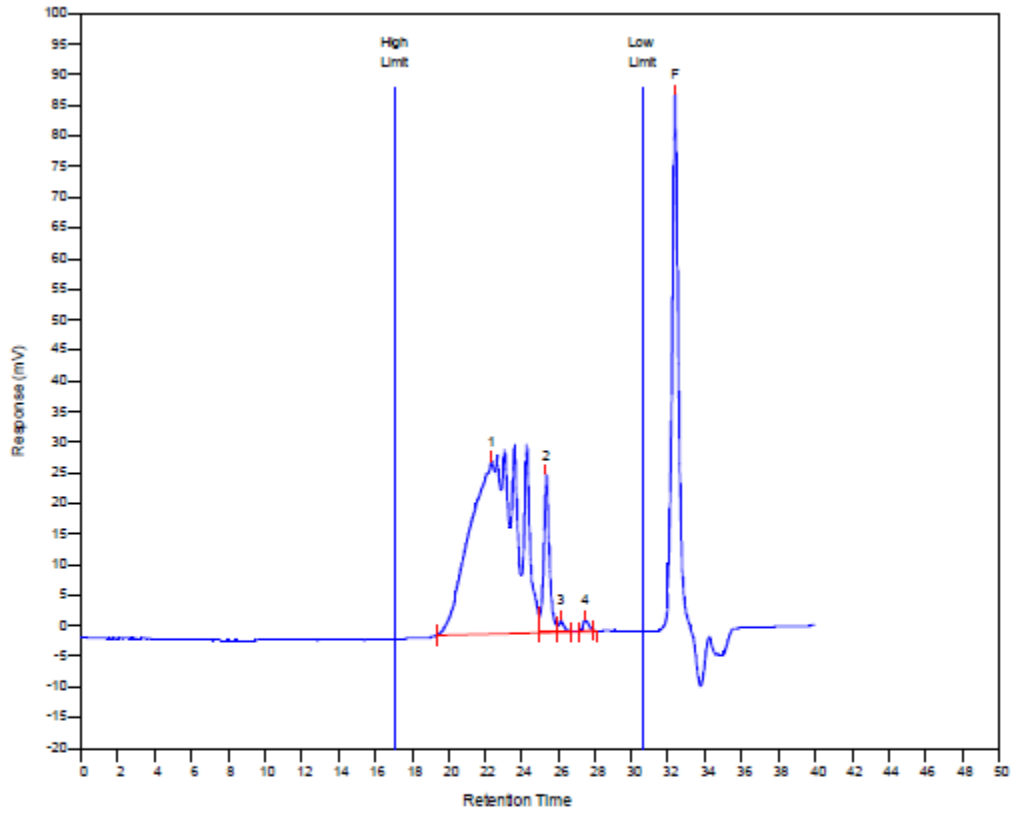
ME8



MW Averages

Peak No	Mp	Mn	Mw	Mz	Mz+1	Mv	PD
1	4064	2969	4220	5854	7647	4006	1.42135
2	663	655	657	661	664	657	1.00305

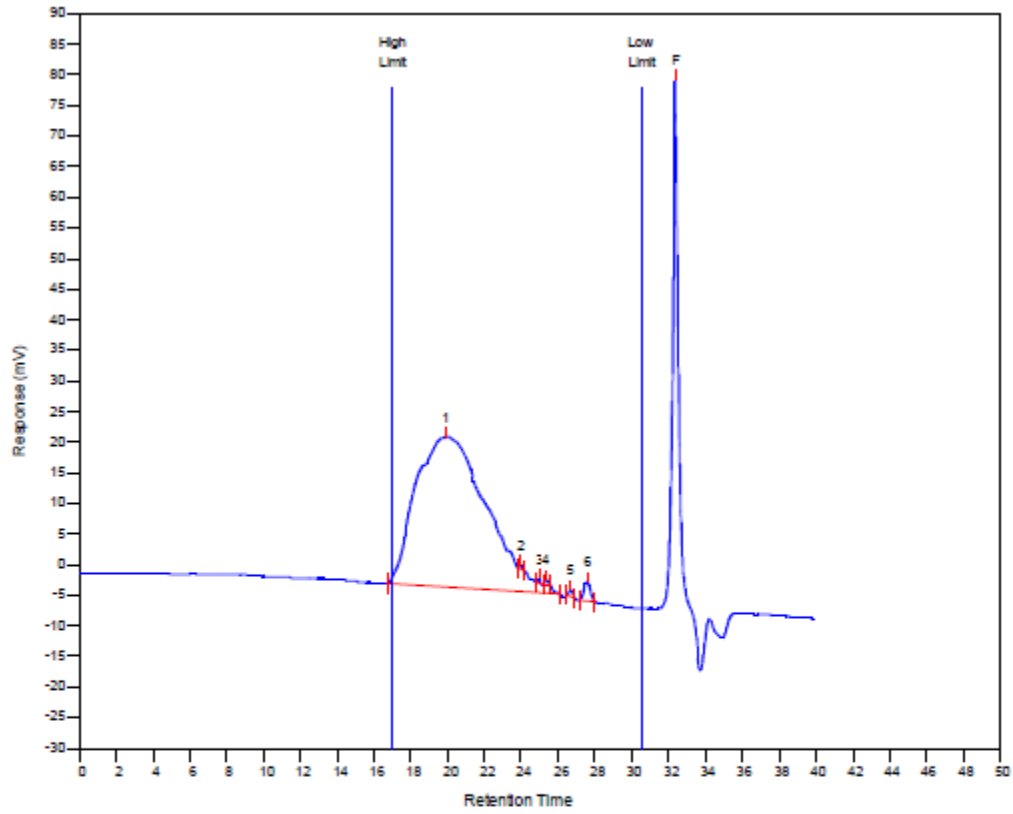
YP40



MW Averages

Peak No	Mp	Mn	Mw	Mz	Mz+1	Mv	PD
1	2347	4538	6439	9413	13041	6077	1.41891
2	1507	1505	1483	1503	1509	1477	0.985382
3	1106	1128	1053	1095	1098	1037	0.933511
4	651	639	641	644	646	640	1.00313

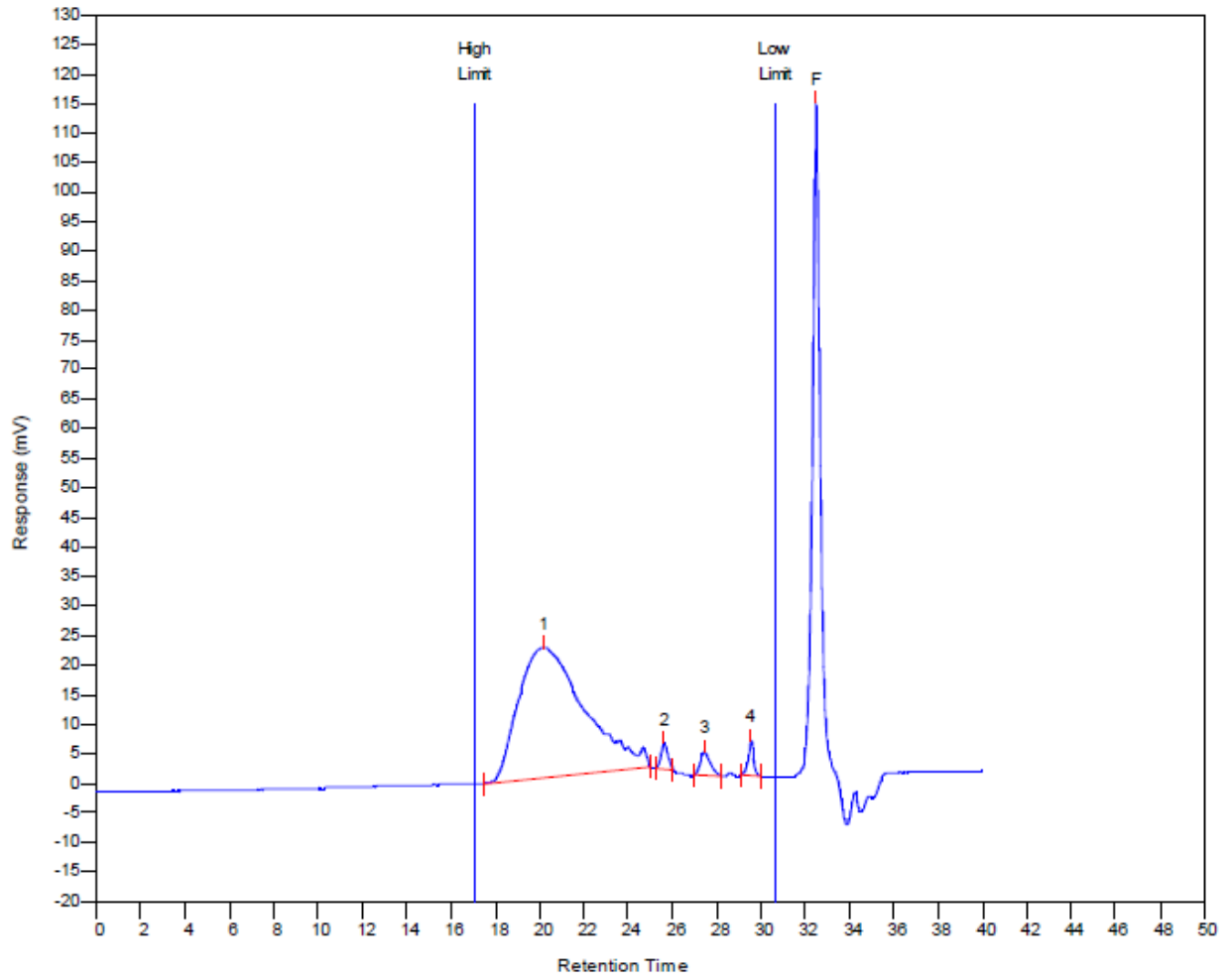
YP41



MW Averages

Peak No	Mp	Mn	Mw	Mz	Mz+1	Mv	PD
1	24785	10873	38211	100440	169109	31954	3.5143
2	2612	2651	2594	2624	2626	2581	0.978499
3	1758	1763	1749	1758	1759	1745	0.992059
4	1497	1498	1485	1494	1495	1482	0.991322
5	885	893	887	892	893	886	0.993281
6	612	624	626	629	631	625	1.00321

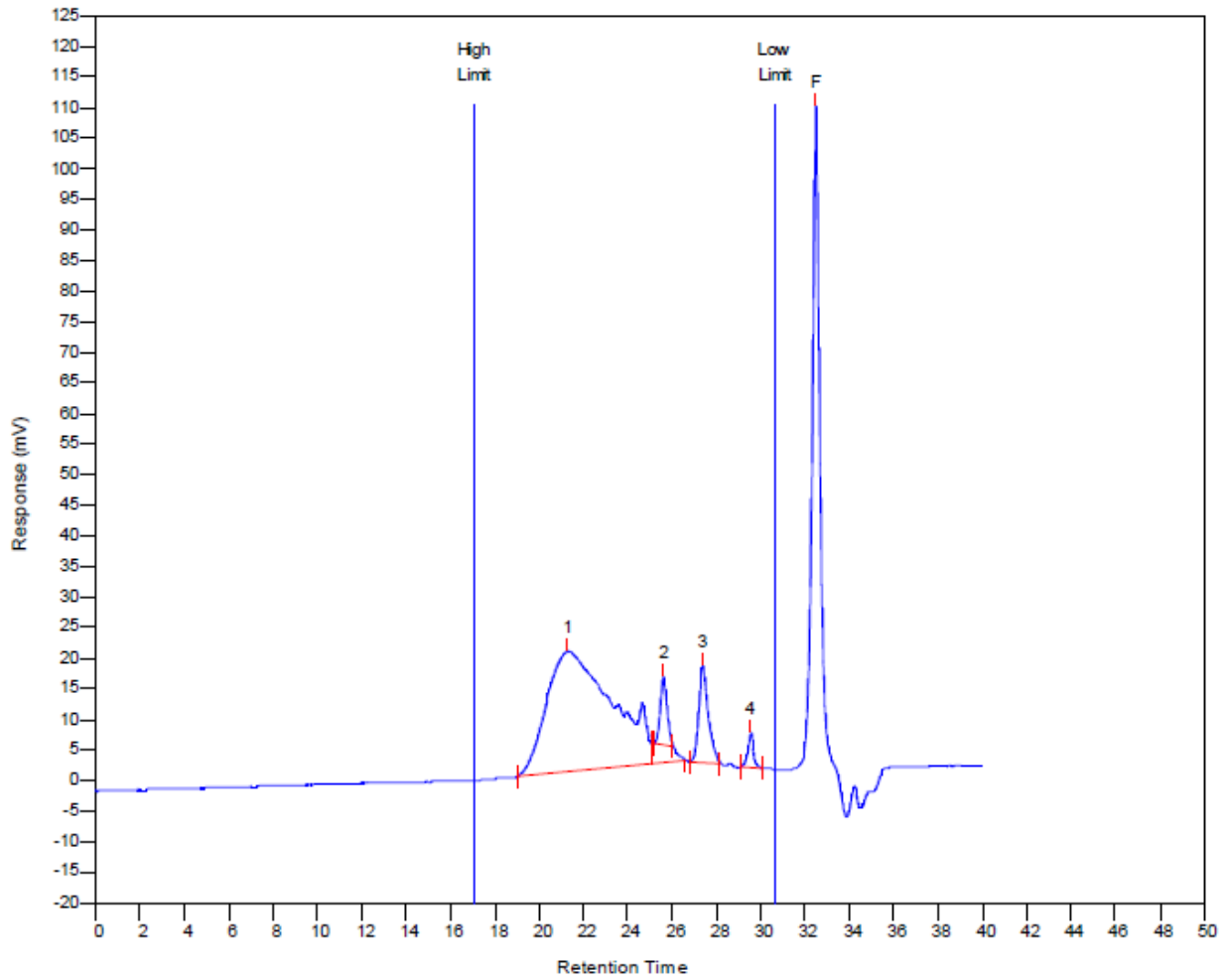
YP42



MW Averages

Peak No	Mp	Mn	Mw	Mz	Mz+1	Mv	PD
1	24722	10420	24572	46495	70012	21925	2.35816
2	1349	1345	1348	1353	1358	1347	1.00223
3	656	646	651	656	661	650	1.00774
4	268	268	269	270	271	268	1.00373

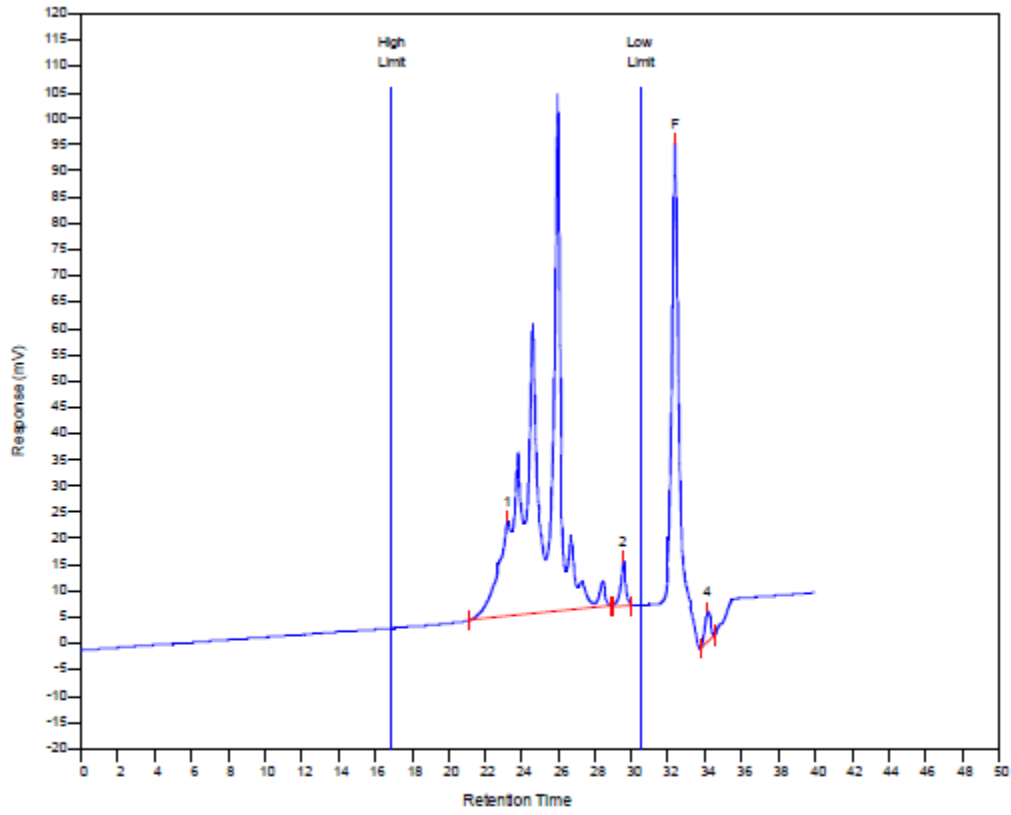
YP43



MW Averages

Peak No	Mp	Mn	Mw	Mz	Mz+1	Mv	PD
1	11014	5546	9613	15345	21263	8875	1.73332
2	1367	1354	1357	1362	1367	1356	1.00222
3	674	661	666	671	676	665	1.00756
4	268	267	268	269	271	268	1.00375

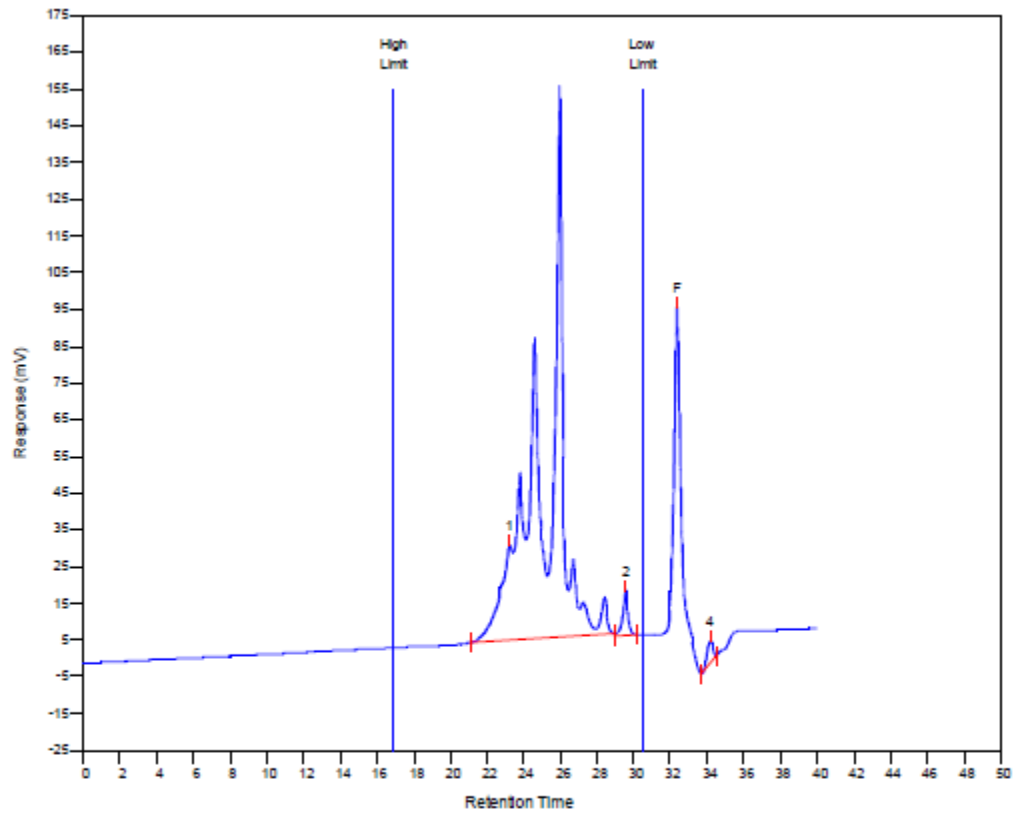
YP44



MW Averages

Peak No	Mp	Mn	Mw	Mz	Mz+1	Mv	PD
1	1163	1508	2033	2781	3704	1040	1.34814

YP45



MW Averages

Peak No	Mp	Mn	Mw	Mz	Mz+1	Mv	PD
1	1170	1470	1992	2738	3685	1899	1.3551
2	252	254	255	257	259	254	1.00394

